Theoretical Aspects of Multicomponent Adsorption Equilibria

Part I: Development of a Computationally Fast Adsorption Isothem Model that can be Applied to Systems Which Demonstrate Energetic Heterogeneity

RICHARD A. MATUSZKO

Geo-Centers, Inc.
Fort Washington, MD

ROBERT A. LAMONTAGE

Chemical Dynamics and Diagnostics Branch
Chemistry Division

19970527 115

April 30, 1997

DTIC QUALITY INSPECTED 1

REPORT DOCUMENTATION PAGE

Public reporting burden for this collection of information is estimated to average 1 hour per response, including the time for reviewing instructions, searching existing data sources, gathering and maintaining the data needed, and completing and reviewing the collection of information. Send comments regarding this burden estimate or any other aspect of this collection of information, including suggestions for reducing this burden, to Washington Headquarters Services, Directorate for Information Operations and Reports, 1215 Jefferson Davis Highway, Suite 1204, Arlington, VA 22202-4302, and to the Office of Management and Budget. Paperwork Reduction Project (0704-0188), Washington, DC 20503.

1. AGENCY USE ONLY (Leave Blank)	2. REPORT DATE April 30, 1997	3. REPORT TYPE AND DATES COVERED Final Report

4. TITLE AND SUBTITLE

Theoretical Aspects of Multicomponent Adsorption Equilibria
Part I: Development of a Computationally Fast Adsorption Isotherm Model that can be
Applied to Systems Which Demonstrate Energetic Heterogeneity

5. FUNDING NUMBERS

PE - 63514N
PR - 30384-05

6. AUTHOR(S)

Richard A. Matuszko* and Robert A. Lamontagne

7. PERFORMING ORGANIZATION NAME(S) AND ADDRESS(ES)

Naval Research Laboratory
Washington, DC 20375-5320

8. PERFORMING ORGANIZATION REPORT NUMBER

NRL/MR/6116--97-7946

9. SPONSORING/MONITORING AGENCY NAME(S) AND ADDRESS(ES)

Naval Sea Systems Command
Washington, DC 20362-5101

10. SPONSORING/MONITORING AGENCY REPORT NUMBER

11. SUPPLEMENTARY NOTES

*Geo-Centers, Inc.
Fort Washington, MD

12a. DISTRIBUTION/AVAILABILITY STATEMENT

Approved for public release; distribution unlimited.

12b. DISTRIBUTION CODE

13. ABSTRACT (Maximum 200 words)

Theoretical aspects of multicomponent adsorption equilibria are investigated with a focus on the thermodynamically based Adsorbed Solution Theory (AST). This report details the development of a computationally fast, heterogeneous, binary adsorption relation using the Langmuir isotherm with the Ideal AST (IAST) as the local, single component and mixture adsorption models. Equations are developed for binary systems which display both equal and unequal saturation/monolayer coverages. Additionally, equations for random and perfectly correlated heterogeneous site matching are developed. Theoretical results plotted as deviations from exact solutions indicate that the developed equations generate consistently better results than analogous homogeneous relations.

14. SUBJECT TERMS

Adsorption	Multicomponent adsorption	Adsorbate
Adsorption solution theory	Langmuir techniques	Adsorbent
Carbon	Adsorption equilibria	
Monolayer coverages	Dynamic adsorption	

15. NUMBER OF PAGES

50

16. PRICE CODE

17. SECURITY CLASSIFICATION OF REPORT UNCLASSIFIED	18. SECURITY CLASSIFICATION OF THIS PAGE UNCLASSIFIED	19. SECURITY CLASSIFICATION OF ABSTRACT UNCLASSIFIED	20. LIMITATION OF ABSTRACT UL

TABLE OF CONTENTS

NOMENCLATURE

A_s	=	Area of the Adsorbent
b	=	Langmuir isotherm fitting parameter (1/MPa)
$F(\epsilon)$	=	Cumulative (integral) energy distribution
$f(\epsilon)$	=	Single probability density function
$g(\epsilon_1,\epsilon_2)$	=	Joint probability density function
H, L	=	Exponential curve fitting parameters
K, u	=	Freundlich parameters
m	=	σ_2^2/σ_1^2
N	=	Global amount adsorbed (moles/kg)
n	=	Amount adsorbed in local homogeneous patch (moles/kg)
P	=	Partial pressure (MPa)
Q	=	Saturation adsorption value (moles/kg)
R	=	Universal gas constant (kJ/mole•K or MPa•L/mole•K)
R_i	=	Constant separation factor isotherm parameter
T	=	Temperature (K)
X	=	Adsorbed phase mole fraction
Y	=	Vapor phase mole fraction
Z	=	Total number of components in the mixture

GREEK LETTERS

γ_i	=	Activity coefficient in the adsorbed phase
ϵ	=	Adsorption site energy (kJ/mole)
μ_p	=	p^{th} central moment of a probability density function
π	=	Spreading pressure
ρ	=	Site matching parameter or covariance of the probability density function
σ	=	Square root of the variance of a probability density function
σ^e	=	Excess area of mixing (kg/mole)
ϕ	=	Fugacity coefficient
ψ	=	Spreading pressure function $\pi A_s/RT$ (moles/kg)

THEORETICAL ASPECTS OF MULTICOMPONENT ADSORPTION EQUILIBRIA

INTRODUCTION

The need exists for a method to accurately model mixture adsorption equilibria. This need arises not only from an academic desire to understand the fundamentals of the adsorption process, but also from the more pragmatic requirement to provide the nucleus of mathematical models which describe dynamic adsorption systems. In the course of generating results for a dynamic adsorption system using accepted mathetical models, adsorption iostherm relationships are regenerated hundred of thousands of times. This points to the importance of generating equilibrium adsorption data with a minimum of computational burden and a high degree of accuracy.

Several models have been developed to describe adsorption systems. The simpler models often are limited in their applicability and accuracy, while the more complicated systems become too cumbersome or unsolvable under some conditions. Several of the models are ultimately correlative in nature. While these models provide important information in understanding the mixture adsorption process, their utility is limited due to the paucity of, and difficulty in obtaining, mixture adsorption data. As a result, models that can predict mixture adsorption from single component adsorption data are becoming more popular.

This study will investigate one of the more popular mixture adsorption theories, the Adsorbed Solution Theory (AST) (Myers and Prausnitz, 1965), and its ability to predict mixture adsorption from single component data. In an effort to isolate pure theory from the effects and inherent errors associated with experimental data, this work will focus mostly on theoretical manipulations and evaluations of the theory. This report details the development of a computationally fast adsorption isotherm model that can be applied to systems which demonstrate energetic heterogeneity. Since this work focuses primarily on the AST, a background section providing the details of this theory is included below.

1

I: ADSORBED SOLUTION THEORY

BACKGROUND

The Adsorbed Solution Theory as proposed by Myers and Prausnitz (1965) is based on the assumption that an adsorbed mixture can be represented as a homogeneous, well-mixed, two-dimensional phase. This assumption leads to a series of thermodynamic relations confined to a two-dimensional plane. Standard three dimensional properties (Pressure and Volume) are reduced to areal properties (Spreading Pressure and Area). Functions which describe nonidealities, such as activity coefficients and excess volume of mixing, also translate to two dimensional analogs. A consequence of this approach is that adsorbate/adsorbent interactions in the AST are completely separate from adsorbate/adsorbate interactions which are modeled as mixture nonidealties. The theory uses the spreading pressure of the mixture as the reference state. The resulting equations are as follows:

$$\frac{1}{n_{TOT}} = \sum_{i=1}^{z} \frac{X_i}{n_i^o} + \sigma^e \tag{1.1}$$

$$1 = \sum_{i=1}^{z} X_i \tag{1.2}$$

$$P_i \phi_i = X_i P_i^o \gamma_i \phi_i^o \tag{1.3}$$

$$P_i^o = \mathscr{F}_1(n_i^o) \tag{1.4}$$

$$\psi = \mathscr{F}_2(n_i^o) \tag{1.5}$$

$$n_i = X_i n_{TOT} \tag{1.6}$$

The function $\mathscr{F}_1(n_i^o)$ is determined directly from the single component isotherm for each specie. The function $\mathscr{F}_2(n_i^o)$ is found using the following equation:

2

$$\mathscr{F}_2(n_i^\circ) = \int_0^{n_i^\circ} \frac{d\ln P}{d\ln n}\, dn \tag{1.7}$$

Or when ψ is a function of P_i°, the $\mathscr{F}_2$ integral can take the form:

$$\mathscr{F}_2(P_i^\circ) = \int_0^{P_i^\circ} \frac{n}{P}\, dP \tag{1.8}$$

The integrand of Equation 1.7 or 1.8 is obtained using the single component isotherm for each specie using the mixture spreading pressure as the standard state. A more rigorous derivation of the thermodynamics associated with the AST can be found in Van Ness (1969).

If it is assumed that the vapor and adsorbed phases are ideal (Ideal Adsorbed Solution Theory - IAST) σ^e becomes 0 and γ_i, ϕ_i, and ϕ_i° all become 1. The resulting $5Z+2$ unknowns in $4Z+2$ equations can be determined if Z conditions are known (i.e. partial pressures for each component). Thus, the method can predict multi-component adsorption values, requiring only single component isotherm information for each specie in the mixture.

In the IAST, the resultant equations are greatly simplified. However, this simplification restricts the application of the theory to adsorbates that behave ideally as a mixture. In adsorption systems that deviate significantly from ideality, a model which describes the adsorbed phase activity coefficients and excess area of mixing must be employed. Costa *et al.* (1981) developed the Real Adsorbed Solution Theory (RAST) to model non-ideal adsorption systems using liquid phase activity coefficient models. Talu and Zwiebel (1986) followed with a proof that the adsorbed phase activity coefficients must depend on the system spreading pressure in order to be thermodynamically consistent. Gamba *et al.* (1989 and 1990) then modified the RAST to minimize the errors associated with low pressure regions and lack of thermodynamic consistency. However, use of this modified RAST is limited to applications requiring calculations in a small concentration range where binary adsorption data already exist.

II: THE DEVELOPMENT OF A FAST HETEROGENEOUS BINARY ADSORPTION ISOTHERM

BACKGROUND

An important practical purpose for an adsorption equilibrium equation is to aid in the modeling of adsorption-based separation systems. The models that describe such systems

3

accurately are often complex and typically involve several layers of nested iterations. At the root of all the calculations is the equilibrium relation which may get called hundreds of thousands of times in any given simulation. Therefore, a simple, fast equilibrium relation is desired to reduce the computational burden and create a manageable overall model.

In an effort to address the need for a computationally fast equilibrium relation, O'Brien and Myers (1985) developed a fast adsorption equilibrium algorithm (FastIAS) based upon the Ideal Adsorbed Solution Theory (Myers and Prausnitz, 1965). Although this model is many times faster than the analogous iterative solution, it is restricted to homogeneous adsorption. To complicate matters further, the single component isotherm relation used in the FastIAS, the TALAN (Taylor series expansion of the Langmuir isotherm) (O'Brien and Myers, 1984), is a heterogeneous isotherm model. This application of a heterogeneous single component isotherm relation in a homogeneous mixture adsorption model seems somewhat inappropriate. Additionally, since the majority of adsorption systems of interest can be categorized as heterogeneous, a new, fast algorithm is needed. This section details the development of a fast heterogenous binary adsorption equilibrium relation. Because of the need for speed, only those solutions that produce a single analytical equation are sought.

Adsorbent heterogeneity has been historically modelled by describing the surface as either patchwise or randomly heterogeneous (Jaroniec and Madey, 1988, p.8). Patchwise heterogeneity assumes that like sites are grouped together to form independent homogeneous patches, while random heterogeneity assumes that the individual homogeneous sites are ungrouped and randomly distributed across the surface. The patchwise model has been favored by researchers in the past because the location or relative placement of the sites is not needed. In the random model, site layout is needed to determine lateral interactions between nearest neighbors. In the patchwise model, since the patches are homogenous and independent, all nearest neighbors are known to be other homogeneous sites. If, however, lateral interactions are ignored, the two models become identical.

For a patchwise heterogenous adsorbent, Jaroniec and Rudzinski (1975) found that the general equation for heterogeneous adsorption takes on a multiple integral form. In a binary system the equation becomes:

$$N_1 = \int_{\epsilon_2} \int_{\epsilon_1} n_1(T,P_1,P_2,\epsilon_1,\epsilon_2) \, g(\epsilon_1,\epsilon_2) \, d\epsilon_1 \, d\epsilon_2 \qquad (2.1)$$

Where N_1 is the global amount of i adsorbed, ϵ_1 is the energy of adsorption, n_1 is the local amount of i adsorbed for a patch characterized by the adsorption site energies ϵ_1 and ϵ_2, and $g(\epsilon_1, \epsilon_2)$ is the joint probability density function for the distribution of adsorption energies. A similar equation can be used to describe the adsorption of component 2. Since transposing the component subscripts in the equations produces the component 2 analog, the remainder of this

4

work will consider only the component 1 equation.

The choice of the local isotherm function is determined by the type of adsorption (monolayer or multilayer) and lateral interactions that are expected on the homogeneous patch. The majority of past research has focused on monolayer adsorption without lateral interactions (Jaroniec and Madey, 1988, p. 220). While Jaroniec and Madey (1988, pp. 213-215, 220) have investigated heterogenous adsorption using local isotherms with lateral interactions and multi-layer adsorption, the equations are too cumbersome to produce an analytical solution. In addition, as Jaroniec and Madey (1988, p. 220) state, there is no satisfactory theory for multilayer adsorption that can be used as a homogeneous local isotherm. For these reasons, this work will focus on monolayer adsorption with no lateral interactions.

The most common adsorption equation for monolayer adsorption with no lateral interactions is the Langmuir adsorption isotherm. If it is assumed that the saturated molar surface coverage is the same for both components (this can later be modified by adding the $Q_1 \neq Q_2$ correction detailed below), the local isotherm then takes the form:

$$n_1 = \frac{Q b_1 P_1 e^{\epsilon_1/RT}}{1 + b_1 P_1 e^{\epsilon_1/RT} + b_2 P_2 e^{\epsilon_2/RT}} \qquad (2.2)$$

The joint probability density function is typically developed by combining the individual probability density functions with a site matching parameter. The common statistical representation of this site matching parameter is the covariance of the two distributions ρ. ρ can take on any value from -1 to +1 and is a measure of how the individual distribution functions are related: $\rho = -1$ indicates perfect negative correlation, $\rho = 0$ indicates random site matching, $\rho = +1$ indicates perfect positive correlation. Perfect positive correlation means that the site with the highest adsorption energy for component 1 will have the highest adsorption energy for component 2 with each subsequent site behaving in the same manner down to the lowest energy site for each component. Perfect negative correlation means that the site with the highest adsorption energy for component 1 will have the lowest adsorption energy for component 2 with each subsequent site behaving in the same contrary manner. Random site matching means that for each adsorption site, the adsorption energy for component 1 has no bearing on, and is completely uncorrelated with, the adsorption energy for component 2. All other values of ρ indicate varying degrees of positive or negative site matching.

The majority of past research into the predetermined selection of covariance has come from the two research groups associated with Jaroniec and Myers. Valenzuela *et al.* (1988) have indicated that, since most adsorption phenomena are controlled by dispersion forces, adsorbates that are similar in size and shape should behave similarly. Therefore, most mixture adsorption systems, in the absence of chemical interactions, are perfectly correlated ($\rho = 1$).

Indeed, Hoory and Prausnitz (1967) found that, for mixtures of ethane and ethylene on charcoal, a $\rho = 1$ value gave an excellent fit of the data. Jaroniec (Jaroniec and Madey, 1988, pp. 199-202, 203-208) has also investigated perfectly correlated adsorption, but limited their efforts to adsorbates which demonstrate identical single component energy distributions, offset only by the differences in the means of the individual distributions. The remainder of Jaroniec's work in this area focuses on the $\rho = 0$ case.

What follows is an evaluation of the possible solutions to Equation 1. In an effort to be comprehensive, solutions are sought for each type of site matching: $\rho = 0$, $\rho = +1$ ($\rho = -1$ producing mathematically similar results to $\rho = +1$), and also for ρ as a binary fit parameter. In addition, two methods of solution (direct integration and expansion) are investigated. The evaluation is separated by the solution approach and is subdivided by the method of site matching.

THEORY

Direct Integration Solution

A direct, analytical solution from integration is the preferred method of solution for Equation 2.1. Other methods such as numerical integration, mathematical approximations, and expansions prior to integration may introduce unwanted errors into the calculation. Furthermore, a numerical integration or inclusion of an extended series defeats the purpose of developing a fast, analytical solution to the binary heterogeneous adsorption equation.

A direct integration requires the selection of a joint probability density function. The simplest function, the bivariate normal distribution used by Hoory and Prausnitz (1967), takes the form:

$$g(\epsilon_1, \epsilon_2) = \frac{1}{2\pi\sigma_1\sigma_2\sqrt{(1-\rho^2)}} e^{-\frac{\Psi_1^2 - 2\rho\Psi_1\Psi_2 + \Psi_2^2}{2(1-\rho^2)}} \tag{2.3}$$

with:

$$\Psi_1 = \frac{\epsilon_1 - \overline{\epsilon_1}}{\sigma_1} \qquad \Psi_2 = \frac{\epsilon_2 - \overline{\epsilon_2}}{\sigma_2} \tag{2.4}$$

ρ as a Fit Parameter. Allowing ρ to be a fit parameter in the binary heterogeneous adsorption equation is appealing because it removes any presuppositions as to the relative interaction of each component with the surface. It does, however, add the complexity that

6

binary data are required to determine ρ. In the strictest sense, the model becomes a correlative rather than a predictive solution. Substituting Equations 2.2 - 2.4 into Equation 2.1 produces a double integral equation which is horribly complex. However, with a little manipulation and substitution, the inner (component 1) integral can be reduced to the form:

$$\int \frac{e^{(Ax^2 + Bx)}}{F + Ge^{Dx}} dx \tag{2.5}$$

with x representing ϵ_1 and A, B, F, G, and D being complex functions of ϵ_2, ρ, and assorted constants from the above equations. Unfortunately, no analytical solution to this integral has been found.

$\rho = 0$ -- Random Site Matching. If random site matching is assumed ($\rho = 0$), Equation 2.3 takes the form:

$$g(\epsilon_1, \epsilon_2) = \frac{1}{2\pi\sigma_1\sigma_2} e^{-\frac{\Psi_1^2}{2}} e^{-\frac{\Psi_2^2}{2}} = f_1(\epsilon_1)f_2(\epsilon_2) \tag{2.6}$$

Unfortunately, using Equations 2.2 and 2.6 to solve Equation 2.1 gives an equation of the same form as Equation 2.5. As with the case where ρ is a variable, no solution has been found.

$\rho = 1$ -- Perfect Positive Correlation. If perfect positive correlation is assumed ($\rho = +1$), then the joint probability density function becomes the individual probability density function of one of the components. Valenzuela et al. (1988) used this information to simplify Equation 1 to a single integral form with respect to the reference component 1:

$$N_1 = \int_{\epsilon_1} n_1(T, P_1, P_2, \epsilon_1, \epsilon_2^*) f(\epsilon_1) d\epsilon_1 \tag{2.7}$$

Since the energy distributions of the two components are positively correlated, ϵ_2 can be represented as a function of the reference energy ϵ_1. According to Valenzuela et al. (1988), this function (ϵ_2^*) takes the form:

$$F_2(\epsilon_2^*) = F_1(\epsilon_1) \tag{2.8}$$

The function F represents the cumulative (integral) energy distributions for each component. Equation 2.8 states that the value of ϵ_2^* can be found by establishing the ϵ_1 value for a given

7

site, finding the corresponding area under the component 1 probability density function defined by ϵ_1, and choosing the component 2 energy value which gives an equivalent area under the component 2 probability density function. If the energy distributions are balanced around the means (i.e. not skewed), then Equation 2.8 simplifies to the linear form:

$$\epsilon_2^* = \frac{\sigma_2^2}{\sigma_1^2}(\epsilon_1 - \overline{\epsilon_1}) + \overline{\epsilon_2} \qquad (2.9)$$

Jaroniec and Madey (1988, pp. 201-202, 203-208) performed a similar simplification, but restricted the application to identically shaped energy distributions by fixing the slope of the linear relationship to one. Unfortunately, as with the other cases noted above, substituting Equations 2.2 and 2.9 into Equation 2.7 produces the familiar integral form found in Equation 2.5.

O'Brien and Myers Expansion Procedure

A second approach to solving Equation 2.1 follows the Taylor series expansion procedure O'Brien and Myers (1984) used to develop the TALAN single component heterogeneous isotherm. The authors expanded the energy dependence of the local Langmuir isotherm about the mean of the energy distribution. This approach is appealing because it does not require an *a priori* specification of a distribution function. In addition, even though this method uses an expansion to approximate a portion of the equation, the penalty for truncation at each level is well defined. Each additional term represents an additional central moment of the probability density function. Therefore, truncating the series at any given point results in the specification of the general form of the probability density function. For example, truncation of the O'Brien and Myers expansion after the second term (as in the TALAN) fixes the shape of the probability function to the symmetric, normal distribution form. Truncation after the third term allows for skewness. Truncation after the fourth term allows for kurtosis. It should be noted, however, that each additional term in the series may provide a superior fit to the data, but adds an additional fit parameter. And, with each additional fit parameter, it becomes more difficult to determine whether a superior fit is provided because the energy distribution is better described by the additional moments, or because more parameters can make a fundamentally poor model seem better.

To apply the approach of O'Brien and Myers to Equation 2.1, their theory must be extended to account for more than one component. In the case of a binary isotherm, the local (binary) isotherm needs to be expanded about the means of the energy distributions of both components yielding:

8

$$n_1(T,P_1,P_2,\epsilon_1,\epsilon_2) = \sum_{p=0}^{\infty} \sum_{q=0}^{\infty} \frac{n_1^{(p)(q)}(\overline{\epsilon_1},\overline{\epsilon_2})(\epsilon_1 - \overline{\epsilon_1})^p(\epsilon_2 - \overline{\epsilon_2})^q}{(p+q)!} \qquad (2.10)$$

where $n_1^{(p)(q)}$ is the multiple derivative of the local isotherm with respect to ϵ_1 (p^{th} derivative) and ϵ_2 (q^{th} derivative). If we follow O'Brien and Myers, substitute Equation 2.10 into Equation 2.1 and then interchange the order of integration:

$$N_1 = \sum_{p=0}^{\infty} \sum_{q=0}^{\infty} \frac{n_1^{(p)(q)}(\overline{\epsilon_1},\overline{\epsilon_2})}{(p+q)!} \int_{\epsilon_2} \int_{\epsilon_1} (\epsilon_1 - \overline{\epsilon_1})^p (\epsilon_2 - \overline{\epsilon_2})^q g(\epsilon_1,\epsilon_2) d\epsilon_1 d\epsilon_2 \qquad (2.11)$$

And, as with direct integration, the possible solutions can be separated by the method used to match the sites.

ρ as a Fit Parameter. Using the distribution defined in Equation 2.3 and a variable ρ value, $g(\epsilon_1, \epsilon_2)$ cannot be broken into two independent functions of ϵ_1 and ϵ_2. However, the distribution can be divided such that the inner (component 1) integral becomes:

$$(\epsilon_2 - \overline{\epsilon_2})^q f_2(\epsilon_2) \int_{\epsilon_1} (\epsilon_1 - \overline{\epsilon_1})^p g_1(\epsilon_1,\epsilon_2) d\epsilon_1 \qquad (2.12)$$

Since the integral is with respect to ϵ_1, $g_1(\epsilon_1, \epsilon_2)$ becomes essentially $f_1(\epsilon_1)$. Thus, the integral in Equation 2.12 is the pth central moment of $f_1(\epsilon_1)$ or μ_p. Equation 2.11 then becomes:

$$N_1 = \sum_{p=0}^{\infty} \sum_{q=0}^{\infty} \frac{n_1^{(p)(q)}(\overline{\epsilon_1},\overline{\epsilon_2})}{(p+q)!} \int_{\epsilon_2} \mu_p (\epsilon_2 - \overline{\epsilon_2})^q f_2(\epsilon_2) d\epsilon_2 \qquad (2.13)$$

Unfortunately, μ_p is a function of ϵ_2 and therefore cannot be removed from the integral. Thus, no solution to this equation has been found.

ρ=0 — Random Site Matching. If random site matching is assumed, the joint probability density function can be separated into two independent functions as shown in Equation 2.6. These separate functions $f_1(\epsilon_1)$ and $f_2(\epsilon_2)$ can be directly substituted for $g(\epsilon_1,\epsilon_2)$ in Equation 2.11. Following the work-up of Equations 2.12 and 2.13, and recognizing the pth and q^{th} - central moments leads to the equation:

9

$$N_1 = \sum_{p=0}^{\infty} \sum_{q=0}^{\infty} \frac{n_1^{(p)(q)}(\overline{\epsilon_1},\overline{\epsilon_2})\mu_p\mu_q}{(p+q)!} \tag{2.14}$$

μ_p and μ_q are respectively the pth central moment of the component 1 distribution and the qth central moment of the component 2 distribution. Following O'Brien and Myers (1984), $\mu_0 = 1$ and $\mu_1 = 0$, so that Equation 2.14 can be written:

$$N_1 = n_1(\overline{\epsilon_1},\overline{\epsilon_2}) + \sum_{p=2}^{\infty} \frac{n_1^{(p)}(\overline{\epsilon_1})\mu_p}{p!} + \sum_{q=2}^{\infty} \frac{n_1^{(q)}(\overline{\epsilon_2})\mu_q}{q!} + \sum_{p=2}^{\infty}\sum_{q=2}^{\infty} \frac{n_1^{(p)(q)}(\overline{\epsilon_1},\overline{\epsilon_2})\mu_p\mu_q}{(p+q)!} \tag{2.15}$$

The sums can be extended knowing that μ_2/σ^2 is the variance of the distribution, while μ_3/σ^3 represents the skewness and μ_4/σ^4 represents the kurtosis.

Using Equation 2.2 for the local isotherm and following O'Brien and Myers (1984) in their development of the TALAN (truncating the sums after the second terms) gives:

$$N_1 = Q(\frac{x}{\xi} + \frac{x(1+y)(1-x+y)\sigma_1^2 + xy(y-x-1)\sigma_2^2}{2R^2T^2\xi^3}) \tag{2.16}$$

where:

$$x = P_1 b_1 e^{\frac{\overline{\epsilon_1}}{RT}} \qquad y = P_2 b_2 e^{\frac{\overline{\epsilon_2}}{RT}} \tag{2.17}$$

$$\xi = 1 + x + y$$

It can be seen that Equation 2.16 reduces to the TALAN for single component ($P_2 = y = 0$):

$$N_1 = Q(\frac{x}{(1+x)} + \frac{x(1-x)\sigma_1^2}{2R^2T^2(1+x)^3}) \tag{2.18}$$

Indeed, fitting each component to a TALAN isotherm gives the parameters (b, Q, $\overline{\epsilon}$, and σ) for the binary equation. In addition, assuming a homogeneous surface ($\sigma_1 = \sigma_2 = 0$, $\overline{\epsilon_1} = \epsilon_1$, and $\overline{\epsilon_2} = \epsilon_2$) yields the familiar Langmuir (Equation 2.2) form for both binary and single component systems.

ρ=1 – Perfect Positive Correlation. As shown above, in the case of perfect positive correlation, Equation 2.1 simplifies to Equation 2.7. If Equation 2.9 is used to replace the ϵ_2^* dependence, Equation 2.7 can be expanded a single time about the mean of the component 1 energy distribution giving:

$$N_1 = \sum_{p=0}^{\infty} \frac{n_1^{(p)}(\overline{\epsilon_1}, \overline{\epsilon_2})}{p!} \int_{\epsilon_1} (\epsilon_1 - \overline{\epsilon_1})^p f(\epsilon_1) d\epsilon_1 \qquad (2.19)$$

The integral in Equation 2.19 is the pth-central moment of the component 1 energy distribution. To evaluate Equation 2.19, Equation 2.2 is used as the local isotherm. Prior to differentiation in Equation 2.19, the ϵ_2 dependence is replaced in Equation 2.2 using the ϵ_2^* function in Equation 2.9. The sum is then evaluated at $\overline{\epsilon_1}$ and $\overline{\epsilon_2}$. Truncating the sum after the second term gives:

$$N_1 = Q(\frac{x}{\xi} + \frac{x\sigma_1^2}{2R^2T^2\xi}(1 - \frac{3x + my(m + 2)}{\xi} + \frac{2(x + my)^2}{\xi^2})) \qquad (2.20)$$

where:

$$x = P_1 b_1 e^{\frac{\overline{\epsilon_1}}{RT}} \qquad y = P_2 b_2 e^{\frac{\overline{\epsilon_2}}{RT}}$$

$$\qquad (2.21)$$

$$m = \frac{\sigma_2^2}{\sigma_1^2} \qquad \xi = 1 + x + y$$

As with the ρ=0 case, Equation 2.20 reduces to the TALAN (Equation 2.18) for single component ($P_2 = y = 0$), and to the basic Langmuir for a homogeneous surface ($\sigma_1 = \sigma_2 = 0$, $\overline{\epsilon_1} = \epsilon_1$, and $\overline{\epsilon_2} = \epsilon_2$).

Binary Systems with Different Molar Monolayer Coverages (Q1 ≠ Q2)

Equations 2.16 and 2.20 represent analytical solutions for a binary heterogeneous system which adsorbs locally as a monolayer without lateral interactions. These solutions cannot, however, be applied when the molar monolayer coverages for the two components are not equal. LeVan and Vermeulen (1981) addressed this problem with binary homogeneous adsorption using a Taylor series expansion about the mean of the two different saturation (monolayer) coverages. Frey and Rodrigues (1994) extended this solution to allow for more than two components. Since this research is focusing on binary adsorption, only the LeVan and Vermeulen, binary solution will be considered here. The equations developed from the LeVan and Vermeulen effort include both a two-term and three-term Taylor expansion. The

11

primary equation for the three-term expansion takes the form:

$$n_1 = \frac{\overline{Q}x}{\xi} + \Delta_{L2}(1 + \Delta_{L3}) \tag{2.22}$$

with:

$$\Delta_{L2} = (Q_1 - Q_2)\frac{xy}{(x + y)^2}\ln(\xi)$$

$$\Delta_{L3} = \frac{(Q_1 - Q_2)}{(Q_1 + Q_2)}\frac{1}{x + y}(\frac{y^2 + 2y - 4x - x^2}{x + y}\ln(\xi) \tag{2.23}$$

$$+ \frac{3x^2 + 4x + xy - 2y - 2y^2}{\xi})$$

$$\overline{Q} = \frac{Q_1x + Q_2y}{x + y} + \frac{2xy(Q_1 - Q_2)^2}{(Q_1 + Q_2)(x + y)^2}((\frac{1}{x + y} + \frac{1}{2})\ln(\xi) - 1) \tag{2.24}$$

For the two term expansion, the following simplifications to the above equations apply:

$$\overline{Q} = \frac{Q_1x + Q_2y}{x + y} \tag{2.25}$$

$$\Delta_{L3} = 0$$

This analytical solution for different monolayer coverages assumes ideal adsorbed solution theory thermodynamic interactions. As a result, this solution may be used as the local isotherm in the proposed heterogeneous model. The O'Brien and Myers (1984) expansion, detailed in equation 2.11, can be applied using equation 2.22 as the local isotherm, and the ultimate solution obtained. Due to the complexity of the resultant equations, only the two-term Taylor expansion form of Equation 2.22 will be considered.

$\rho=0$ -- **Random Site Matching.** When random site matching is assumed, Equation 2.22 is used for the local isotherm in Equation 2.15. Truncating the expansion after the second term and using the definitions of Equations 2.17, 2.23, 2.24, and 2.25 gives:

$$N_1 = \frac{\overline{Q}x}{\xi} + \Delta_{L2} + \frac{\sigma_1^2}{2R^2T^2}(\alpha+\beta) + \gamma\frac{(Q_1-Q_2)xy}{2R^2T^2(x+y)^2} \qquad (2.26)$$

where:

$$\alpha = \frac{3x^2(Q_1-\overline{Q})}{(x+y)\xi} + \frac{2x^3(\overline{Q}-Q_1)}{(x+y)^2\xi} + \frac{2x^3(\overline{Q}-Q_1)}{(x+y)\xi^2} + \frac{\overline{Q}x}{\xi} - \frac{3\overline{Q}x^2}{\xi^2} + \frac{2\overline{Q}x^3}{\xi^3} \qquad (2.27)$$

$$\beta = \frac{xy(Q_2-\overline{Q})}{(x+y)\xi} + \frac{2xy^2(\overline{Q}-Q_2)}{(x+y)^2\xi} + \frac{2xy^2(\overline{Q}-Q_2)}{(x+y)\xi^2} - \frac{\overline{Q}xy}{\xi^2} + \frac{2\overline{Q}xy^2}{\xi^3} \qquad (2.28)$$

$$\gamma = (\sigma_1^2+\sigma_2^2)\ln\xi + (x\sigma_1^2+y\sigma_2^2)(\frac{3}{\xi}-\frac{6\ln\xi}{(x+y)}) +$$
$$+(x^2\sigma_1^2+y^2\sigma_2^2)(\frac{6\ln\xi}{(x+y)^2}-\frac{4}{(x+y)\xi}-\frac{1}{\xi^2}) \qquad (2.29)$$

$\rho=+1$ — **Perfect Positive Correlation.** When perfect positive correlation is assumed, Equation 2.22 is used for the local isotherm in Equation 2.19. Truncating the expansion after the second term and using the definitions of Equations 2.21, 2.23, 2.24, and 2.25 gives:

$$N_1 = \frac{\overline{Q}x}{\xi} + \Delta_{L2} + \frac{\sigma_1^2}{2R^2T^2}[\frac{x}{\xi}\alpha + \frac{xy(Q_1-Q_2)\ln\xi}{(x+y)^2}(\beta-\gamma)] \qquad (2.30)$$

where:

$$\alpha = (\overline{Q}+\overline{Q'})(1-\frac{2(x+my)}{\xi}) + (\overline{Q'}+\overline{Q''}) - \frac{\overline{Q}(x+m^2y)}{\xi} + \frac{2\overline{Q}(x+my)^2}{\xi^2} \qquad (2.31)$$

$$\beta = m(m+1)^2\ln(\xi) + \frac{(x+m^2y)+2(x+my)(m+1)}{\xi} - \frac{(x+my)^2}{\xi^2} \qquad (2.32)$$

13

$$\gamma = \frac{4(x+my)^2}{(x+y)\xi} + \frac{2m(2x+3my-y)\ln(\xi)}{(x+y)}$$ (2.33)

$$\overline{Q}' = \frac{Q_1 x + Q_2 my - \overline{Q}(x+my)}{(x+y)}$$ (2.34)

$$\overline{Q}'' = \frac{Q_1 x + Q_2 m^2 y - \overline{Q}(x+m^2 y)}{(x+y)} - \frac{2(x+my)}{(x+y)}\overline{Q}'$$ (2.35)

It can be seen that, with a little mathematical manipulation, Equations 2.26 and 2.30 reduce to the TALAN (Equation 2.18) in the limit of one component ($P_2 = y = 0$), to the Langmuir (Equation 2.2) when the surface is homogeneous ($\sigma_1 = \sigma_2 = 0$, $\bar{\epsilon}_1 = \epsilon_1$, and $\bar{\epsilon}_2 = \epsilon_2$). and to Equations 2.16 and 2.20 when the monolayer coverages are equal ($Q_1 = Q_2 = Q$). These equations may be extended to a higher number of components or to a greater level of complexity in any of the Taylor expansions.

COMPARISONS AND DISCUSSION

Equations 2.16, 2.20, 2.26 and 2.30 represent a step forward in the development of a computationally fast heterogeneous adsorption equation. However, what ultimately determines the utility of the equations and underlying assumptions is the quality of the fit produced when compared with an exact solution. Since a universal exact solution to Equation 1 has not been found, the "exact" solution presented for each case will be one found when assuming specific constraints on the system. What follows is a discussion of how the developed equations compare to the "exact" solutions calculated for each specific case.

Equal Monolayer Coverages: $Q_1 = Q_2$

$\rho = 0$ -- **Random Site Matching.** Exact solutions were generated and compared to the results obtained from Equation 2.16 for a variety of conditions. Results are plotted in Figures 2.1 - 2.3. Results from the Langmuir isotherm (Equation 2.2 with $\bar{\epsilon}_1 = \epsilon_1$ and $\bar{\epsilon}_2 = \epsilon_2$) were also compared with the exact solutions. The exact solutions were generated by substituting Equations 2.2 and 2.6 into Equation 2.1 and integrating the results numerically using the Euler method. It should be noted that the "exact" solution is constrained by the assumptions inherent in Equations 2.2 and 2.6 (i.e. local Langmuir isotherm and Gaussian shaped energy distribution curves). The Euler integration was centered on $\bar{\epsilon}$ for each component using 200 integration steps. The selected model isotherm parameters were based on typical values as

14

indicated by O'Brien and Myers (1984) and are listed in Table 2.1. A copy of the BASIC code written to perform the integration and compare the results to the calculated Equation 2.16 and Langmuir results can be found in Appendix A.

TABLE 2.1: Variable values used in numerical calculations

	Component 1	Component 2
T	298 K	298 K
Q	1.0	1.0
$\bar{\epsilon}$	10*RT	12*RT
b	$1.0*e^{-10}$	$1.2*e^{-10}$

Figure 2.1 compares the percent error for Equation 2.16 and the Langmuir isotherm as a function of total system pressure and breadth of the heterogeneous energy distributions (σ/RT). In this plot, σ/RT and the partial pressure for each component are held equal ($Y_1 = 0.5$). As the plot shows, the deviations from the exact solution for Equation 2.16 are consistently smaller than those of the Langmuir equation. While the Langmuir errors get consistently worse with increasing pressure, the Equation 2.16 errors appear oscillatory. It cannot be determined from the plot, however, whether the Equation 2.16 series will ultimately converge at higher pressures.

Figures 2.2 and 2.3 show the dramatic difference between the Equation 2.16 solution and the Langmuir solution. Figure 2.2 gives the Equation 2.16 and Langmuir errors when the energy distributions for both components are held constant and equal ($\sigma/RT = 0.75$) while the relative vapor phase concentrations are varied. Figure 2.3 compares Equation 2.16 and Langmuir errors when Y_1 and σ_1/RT are held constant at 0.5 and 0.75 respectively, and σ_2/RT is varied. In both plots, the Langmuir errors increase consistently with increasing pressure while the Equation 2.16 errors oscillate around 0. As the plots show, for any given point, the errors obtained for the Equation 2.16 solution are approximately an order of magnitude better than those obtained from the Langmuir solution.

$\rho=1$ -- **Perfect Positive Correlation.** Exact solutions were generated and compared to the results obtained from Equation 2.20 for a variety of conditions and plotted in Figures 2.4 - 2.6. The exact solutions were generated by substituting Equations 2.2 and 2.9 into Equation 2.7 and integrating the results numerically using the Euler method. As with the $\rho=0$ case above, the "exact" solution is constrained by the assumptions inherent to Equations 2.2 and 2.9 (i.e. local Langmuir isotherm and Gaussian or non-skewed energy distribution curves). The Euler integration was centered on $\bar{\epsilon}_1$ using 200 integration steps. The selected model isotherm parameters are the same as those used in the $\rho=0$ calculations above, and can be found in Table 2.1. A copy of the BASIC code written to perform the integration and compare the results to the calculated Equation 2.20 and Langmuir results can be found in Appendix B.
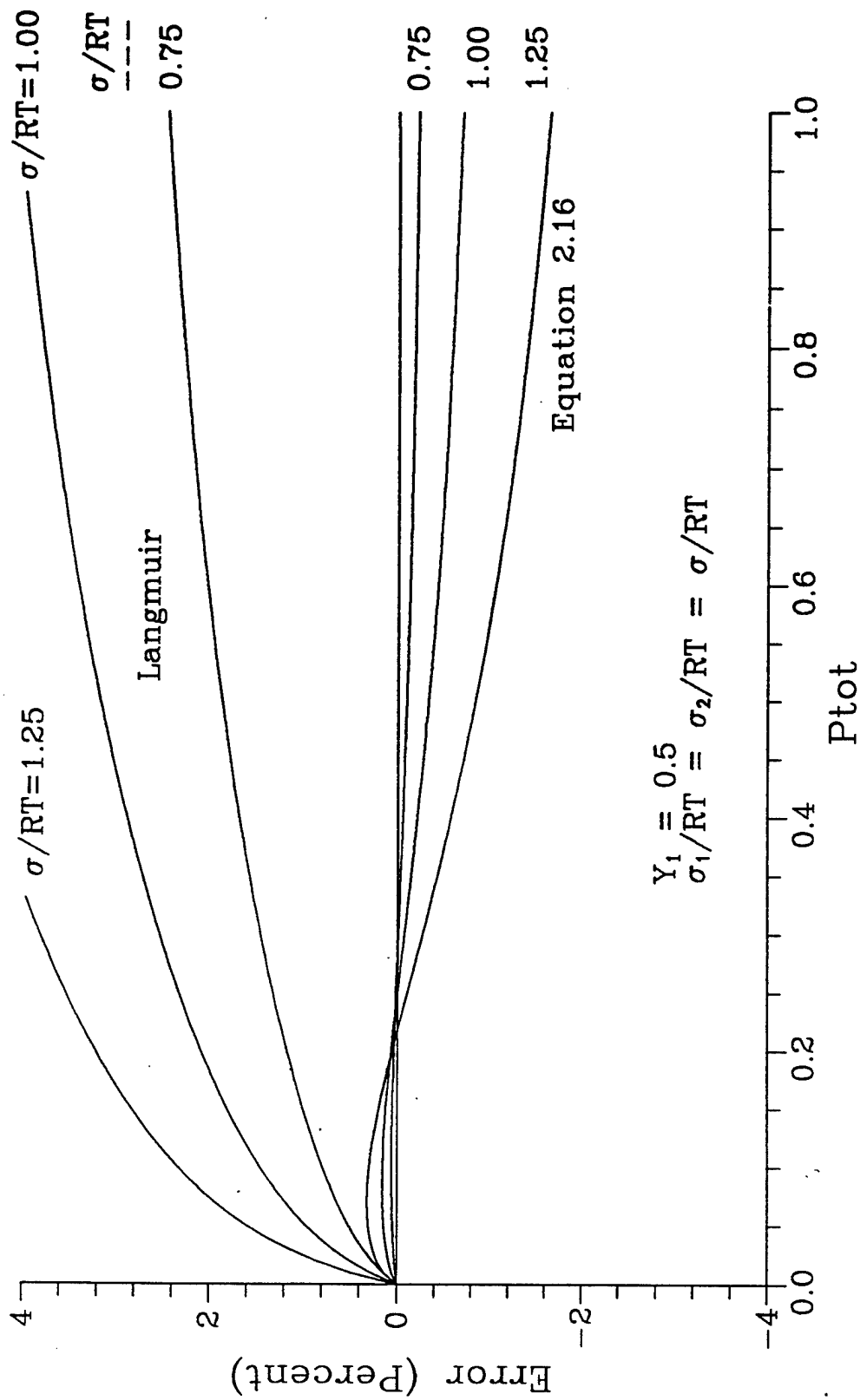
15

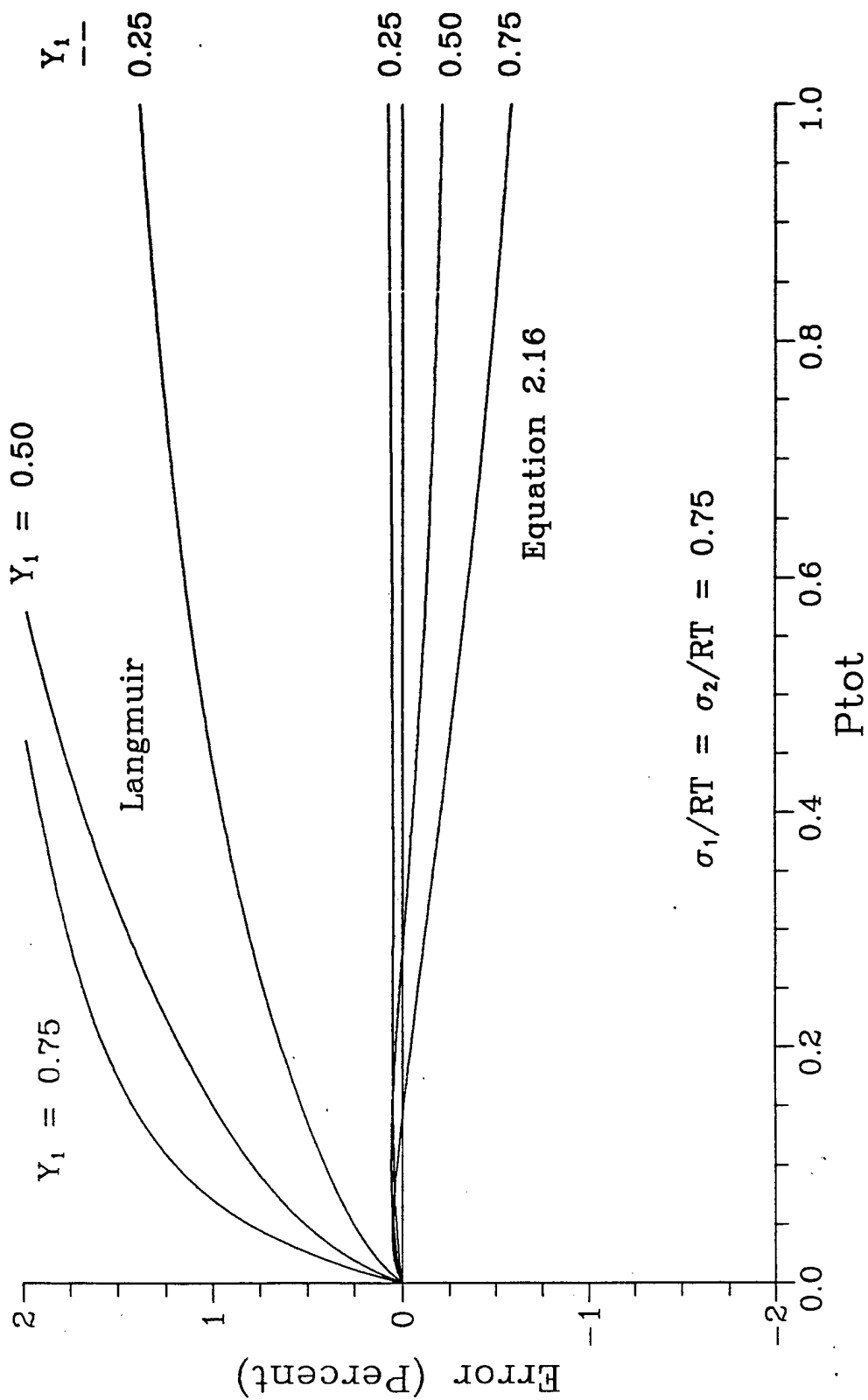FIGURE 2.1: Percent Error for the Langmuir Isotherm and Equation 2.16

FIGURE 2.2: Percent Error for the Langmuir Isotherm and Equation 2.16
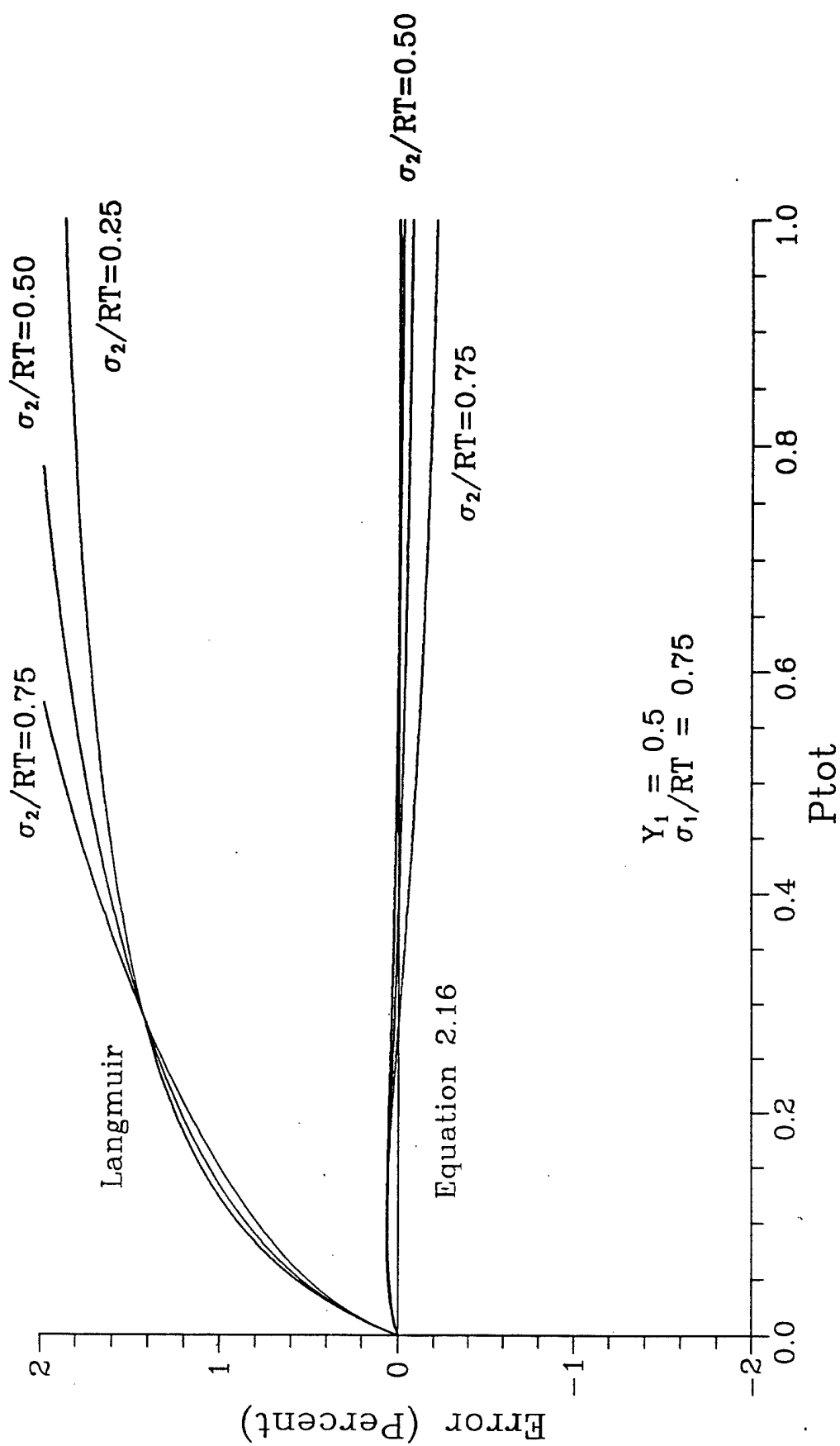
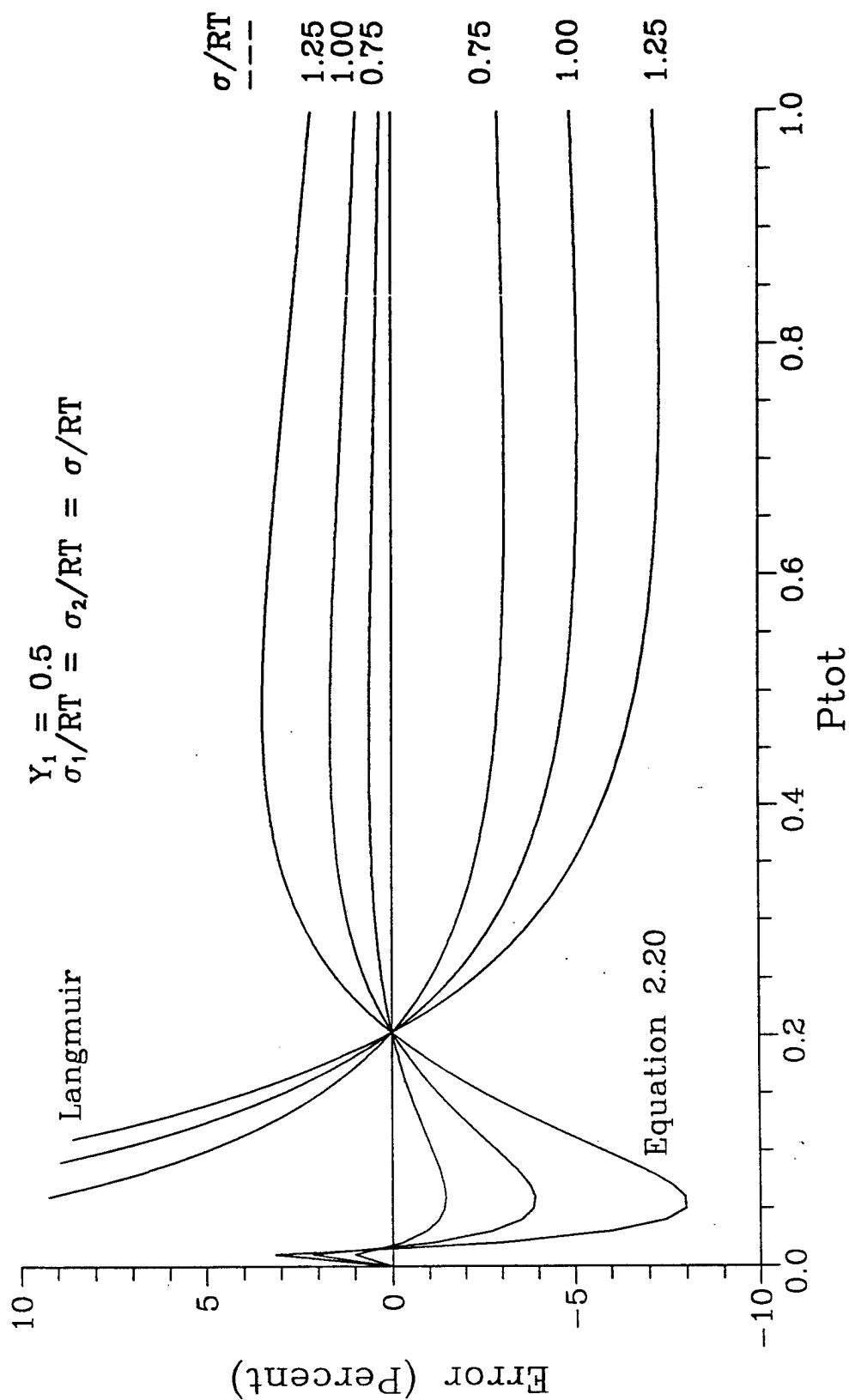FIGURE 2.3: Percent Error for the Langmuir Isotherm and Equation 2.16

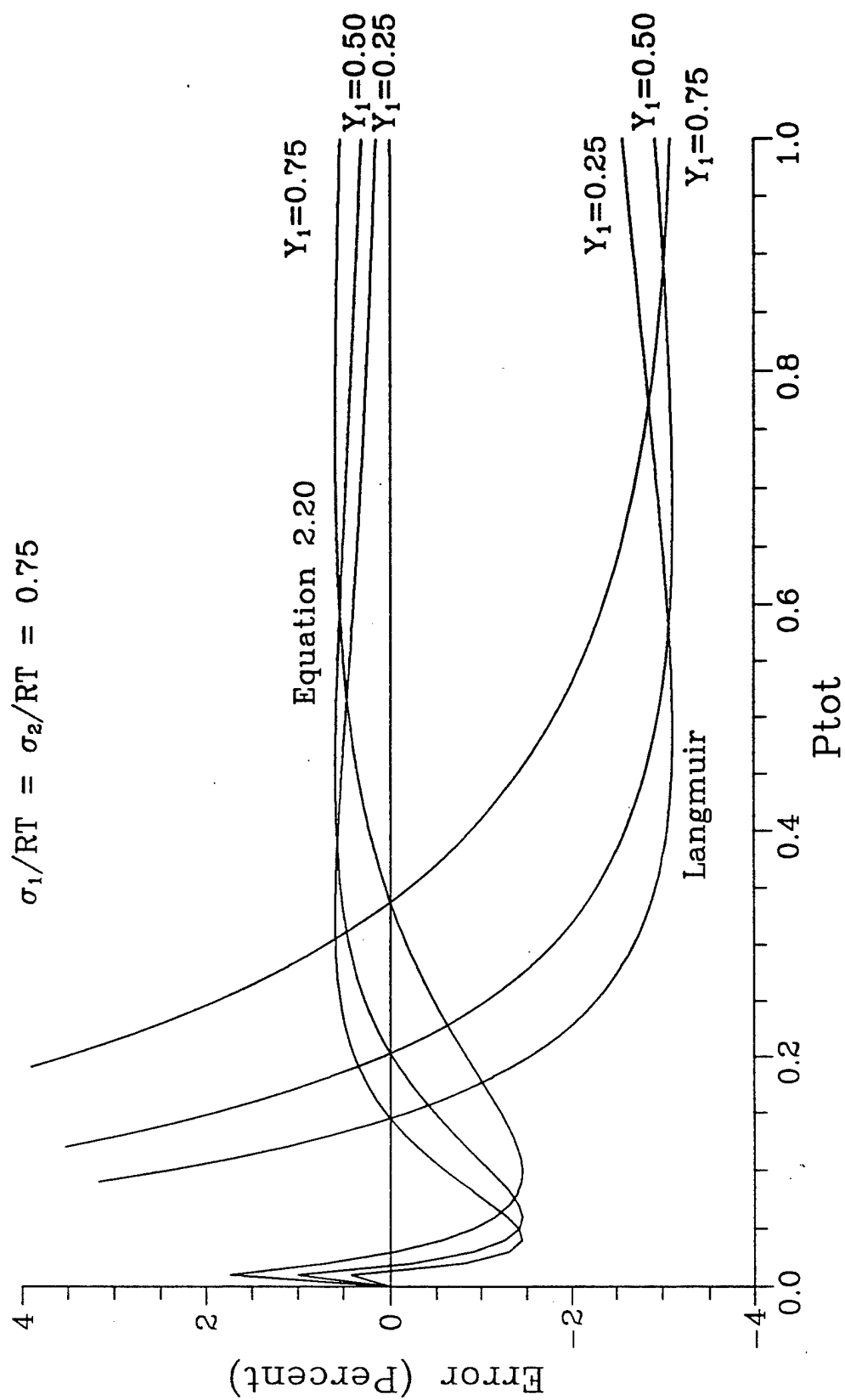FIGURE 2.4: Percent Error for the Langmuir Isotherm and Equation 2.20

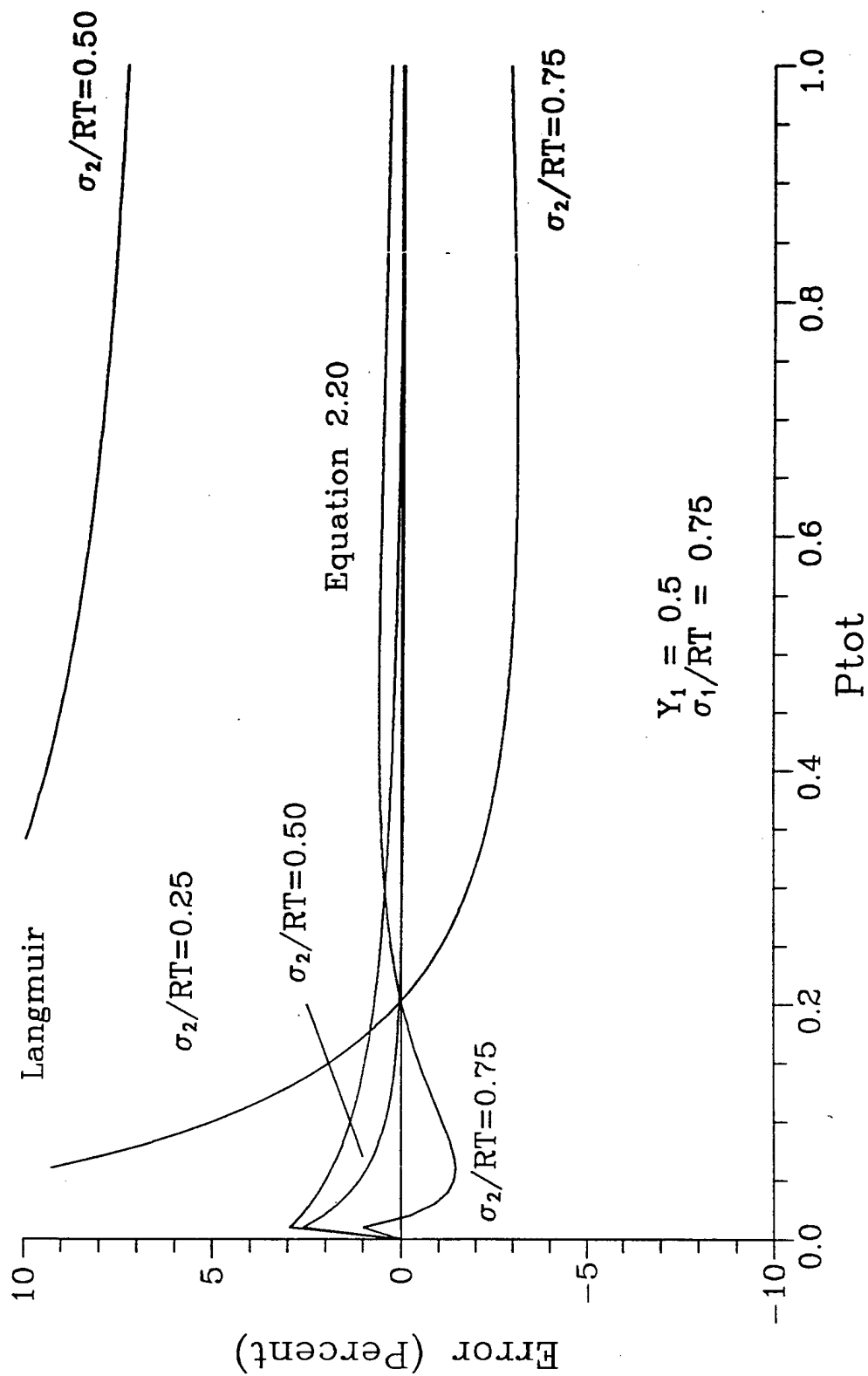FIGURE 2.5: Percent Error for the Langmuir Isotherm and Equation 2.20

20

FIGURE 2.6: Percent Error for the Langmuir Isotherm and Equation 2.20

Figure 2.4 compares the percent error for Equation 2.20 and the Langmuir isotherm as a function of total system pressure and breadth of the heterogeneous energy distributions (σ/RT). In this plot, σ/RT and the partial pressure for each component are held equal ($Y_1 = 0.5$). As the plot shows, the deviations from the exact solution for Equation 2.20 are consistently smaller than those of the Langmuir equation. As would be expected for an expansion solution, the deviations from the exact values are oscillatory with decreasing absolute magnitudes as the breadth of the distribution gets narrower. Although the error gets as high as 8% for the $\sigma/RT = 1.25$ solution, the results still converge with increasing pressure values.

Figure 2.5 shows how Equation 2.20 and the Langmuir isotherm perform when the energy distributions for both components are held constant and equal ($\sigma/RT = 0.75$) while the relative vapor phase concentrations are varied. Once again, Equation 2.20 gives consistently better results than the Langmuir isotherm.

The final plot in this group, Figure 2.6, provides the most insight into the quality of the Equation 2.20 results as compared to those of the Langmuir equation. In this plot, Y_1 and σ_1/RT are held constant at 0.5 and 0.75 respectively, while σ_2/RT is varied. As σ_2/RT drops from 0.75 to 0.25, the Equation 2.20 error shifts upward in the lower pressure region, but converges more rapidly as the pressure is increased. The Langmuir solution, however, is so poor that the $\sigma_2/RT = 0.25$ curve does not fit on the plot.

Unequal Monolayer Coverages: $Q_1 \neq Q_2$

$\rho=0$ -- Random Site Matching. Figures 2.7-2.12 are plots comparing Equation 2.26 results to those obtained from the homogeneous Langmuir solutions of LeVan and Vermeulen (Equation 2.22). The results from each of these equations are plotted as a percentage of error calculated from an "exact" solution. The exact solutions were generated by substituting Equation 2.6 and an ideal adsorbed solution theory, iterative mixture solution based on Equation 2.2, into Equation 2.1 and integrating the results numerically using the Euler method. As with the $Q_1 = Q_2$ case detailed previously, the "exact" solutions are subject to the constraints inherent in Equations 2.2 and 2.6 (i.e. local Langmuir isotherm and Gaussian shaped energy distribution curves). The Euler integration was centered on $\bar{\epsilon}$ for each component using 200 integration steps. The selected model isotherm parameters are listed in Table 2.1. A copy of the BASIC code written to perform the integration, and compare the results to the calculated Equation 2.22 and Equation 2.26 results can be found in Appendix C.

The plots can be divided into two series: Figures 2.7 - 2.9 using $Q_1 = 0.9$ and $Q_2 = 1.1$, and Figures 2.10 - 2.12 using $Q_1 = 0.8$ and $Q_2 = 1.2$. The latter of the two cases should represent a fairly extreme spread in saturation values, with Q_2 being 50% larger than Q_1. As the plots indicate, as values for site energy distribution breadth, vapor phase mole fraction, and site energy distribution ratios are changed,
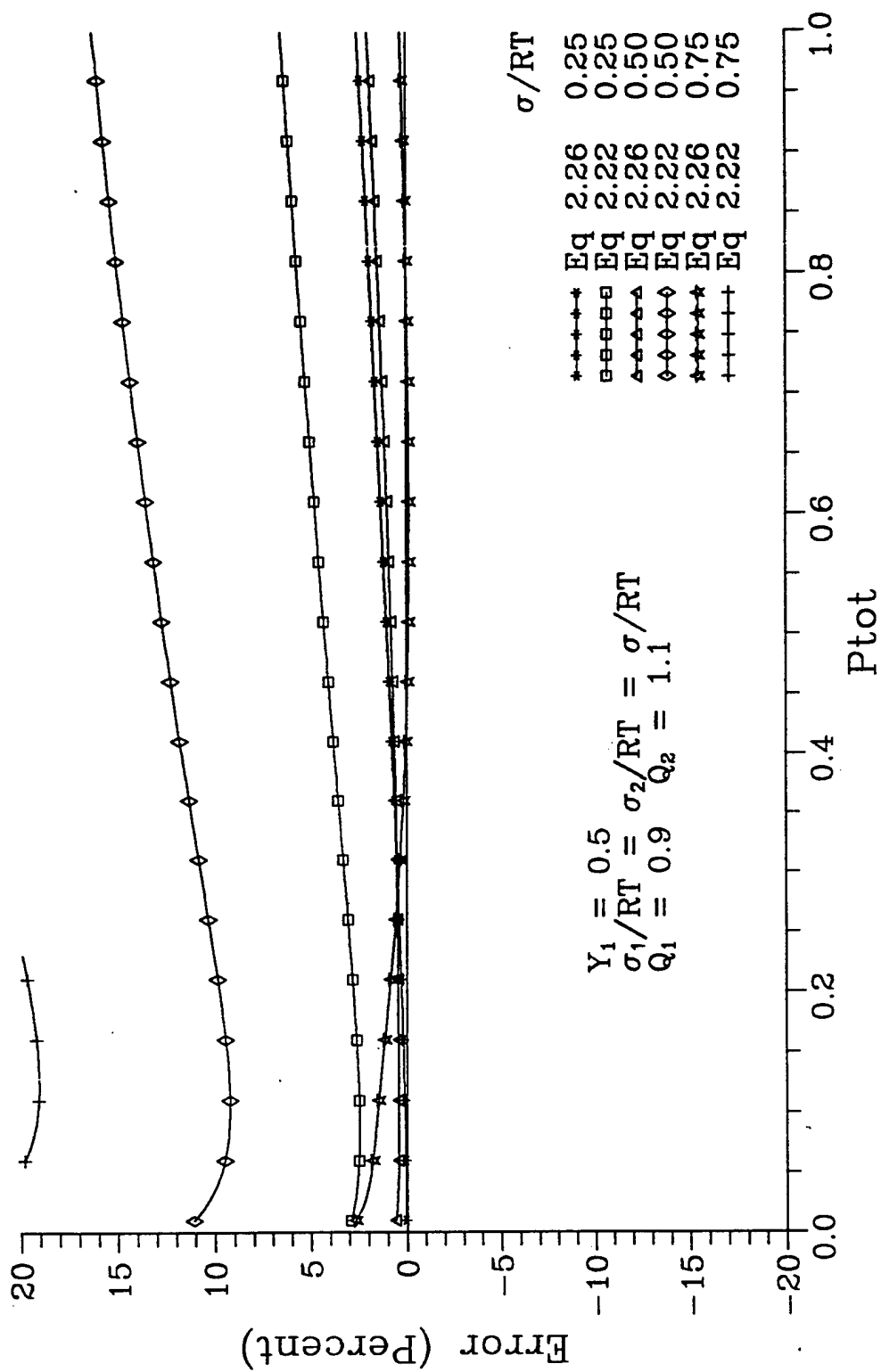
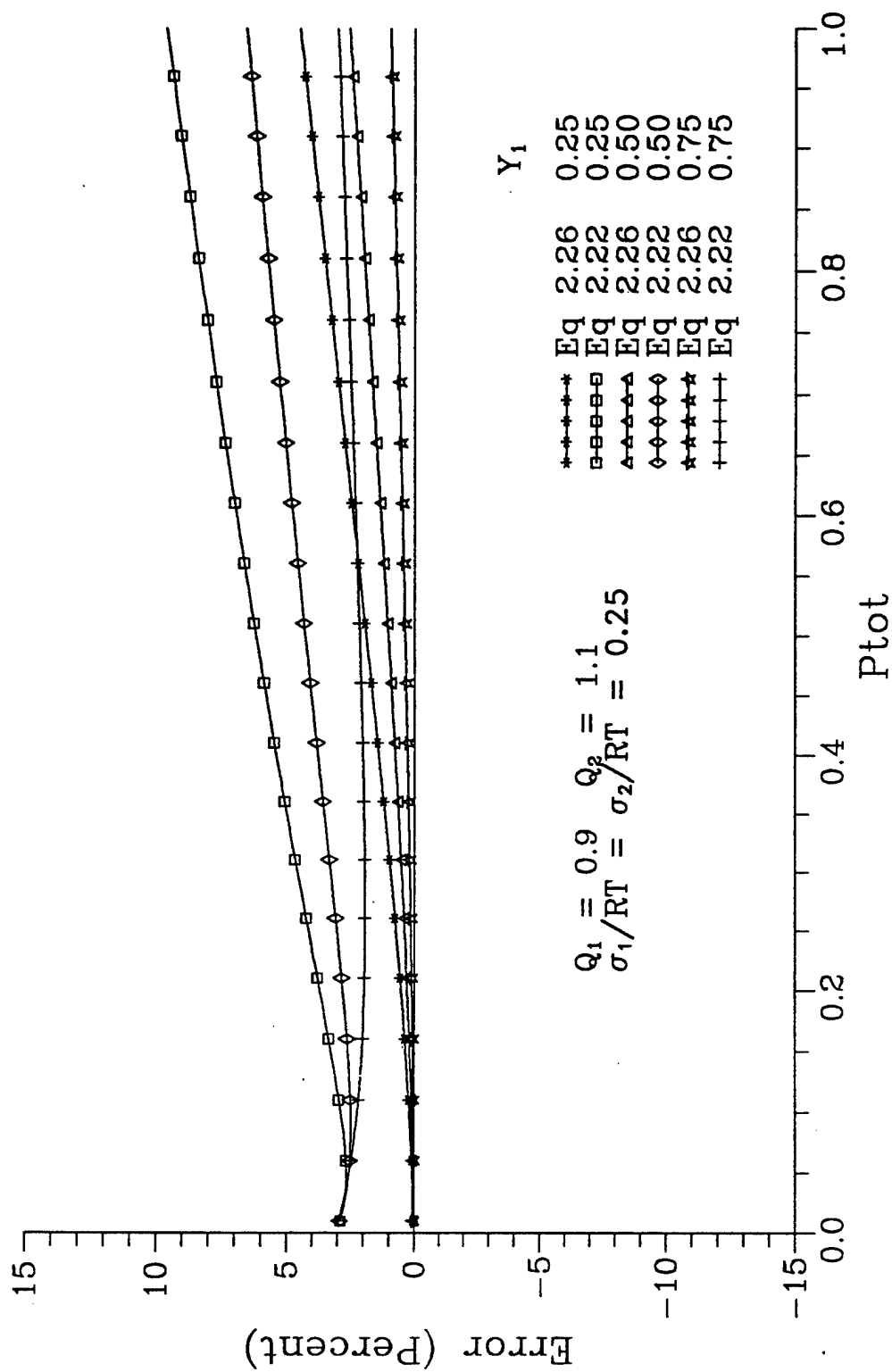FIGURE 2.7: Percent Error Equations 2.22 and 2.26

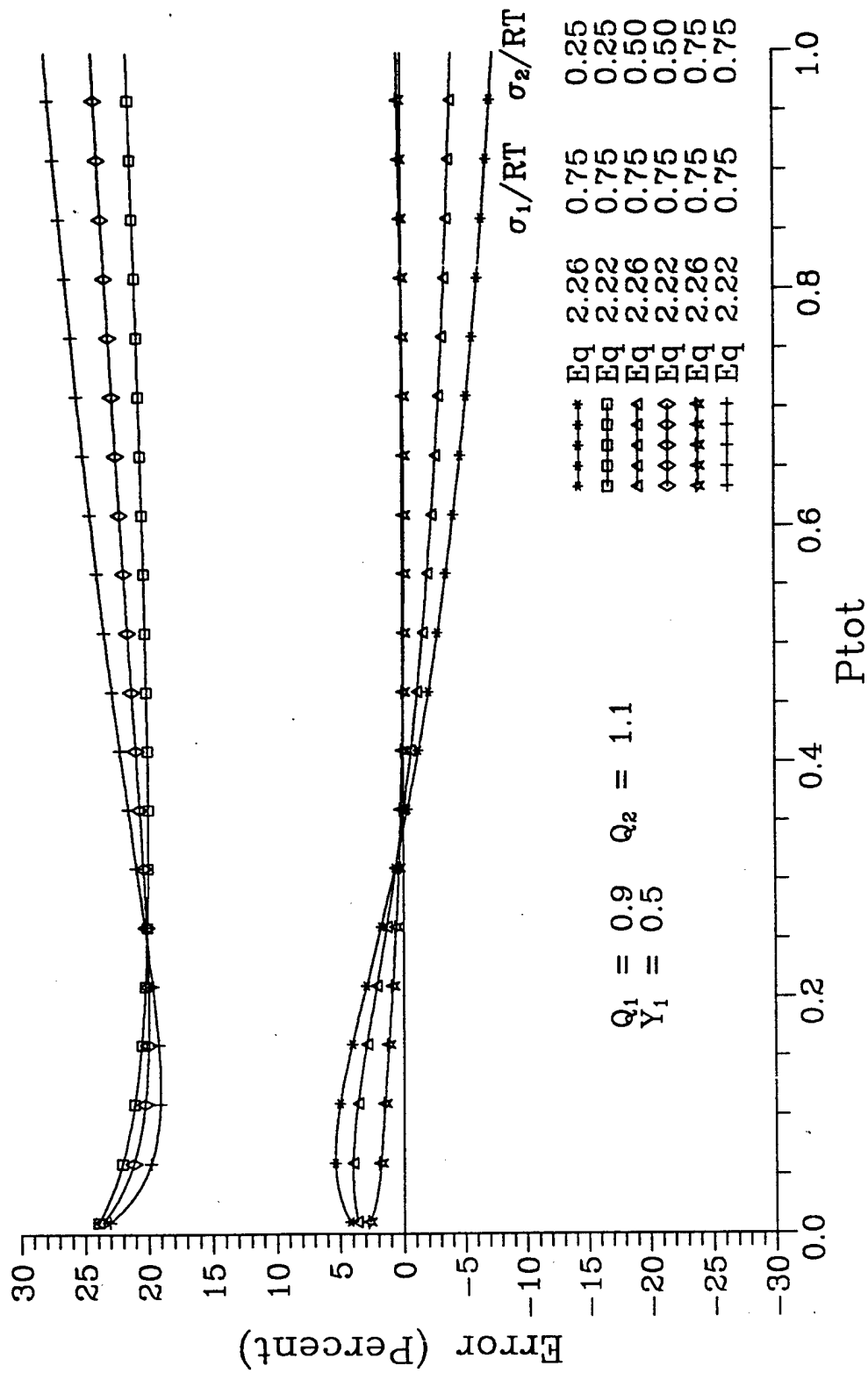FIGURE 2.8: Percent Error Equations 2.22 and 2.26

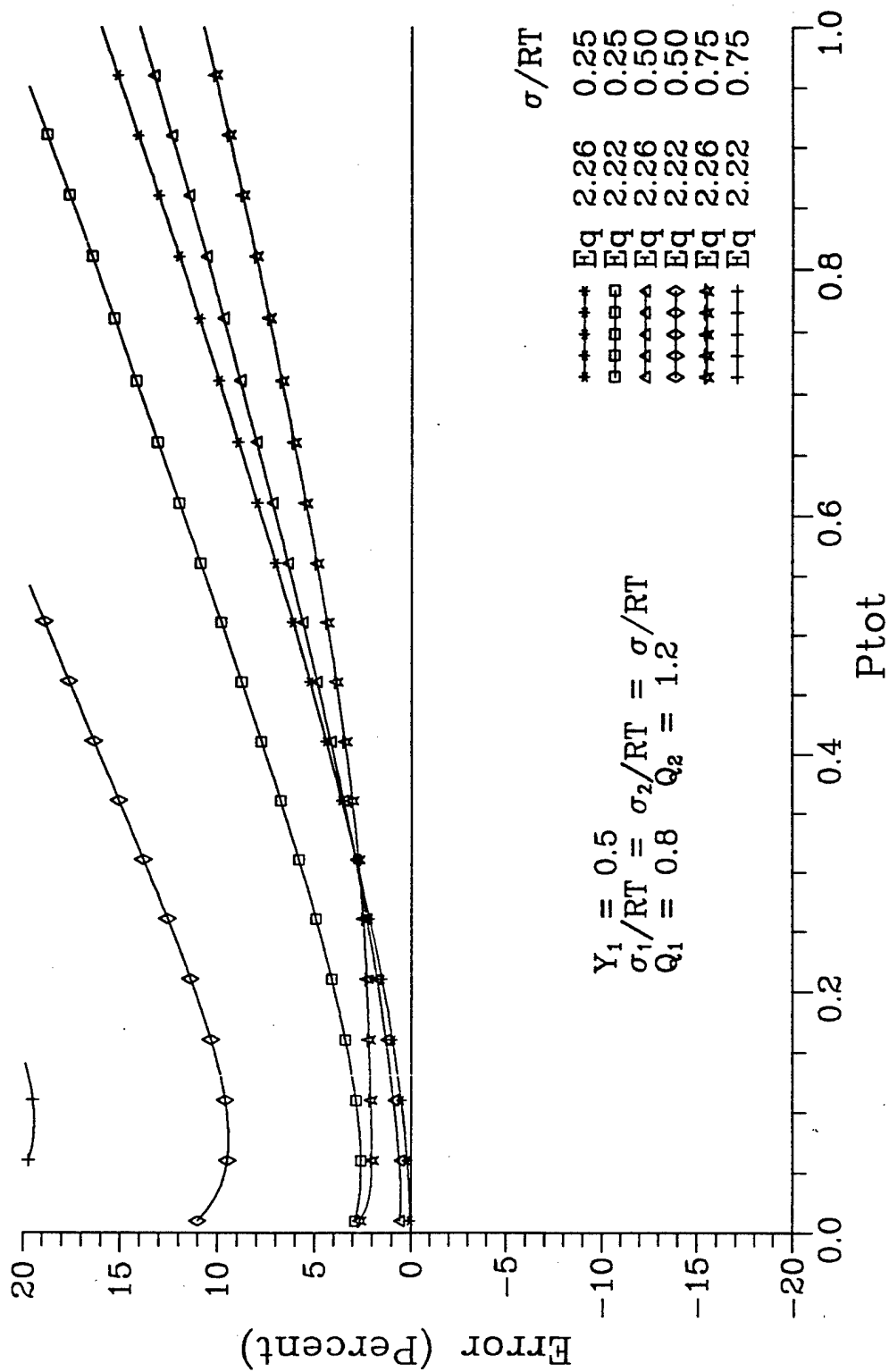FIGURE 2.9: Percent Error Equations 2.22 and 2.26

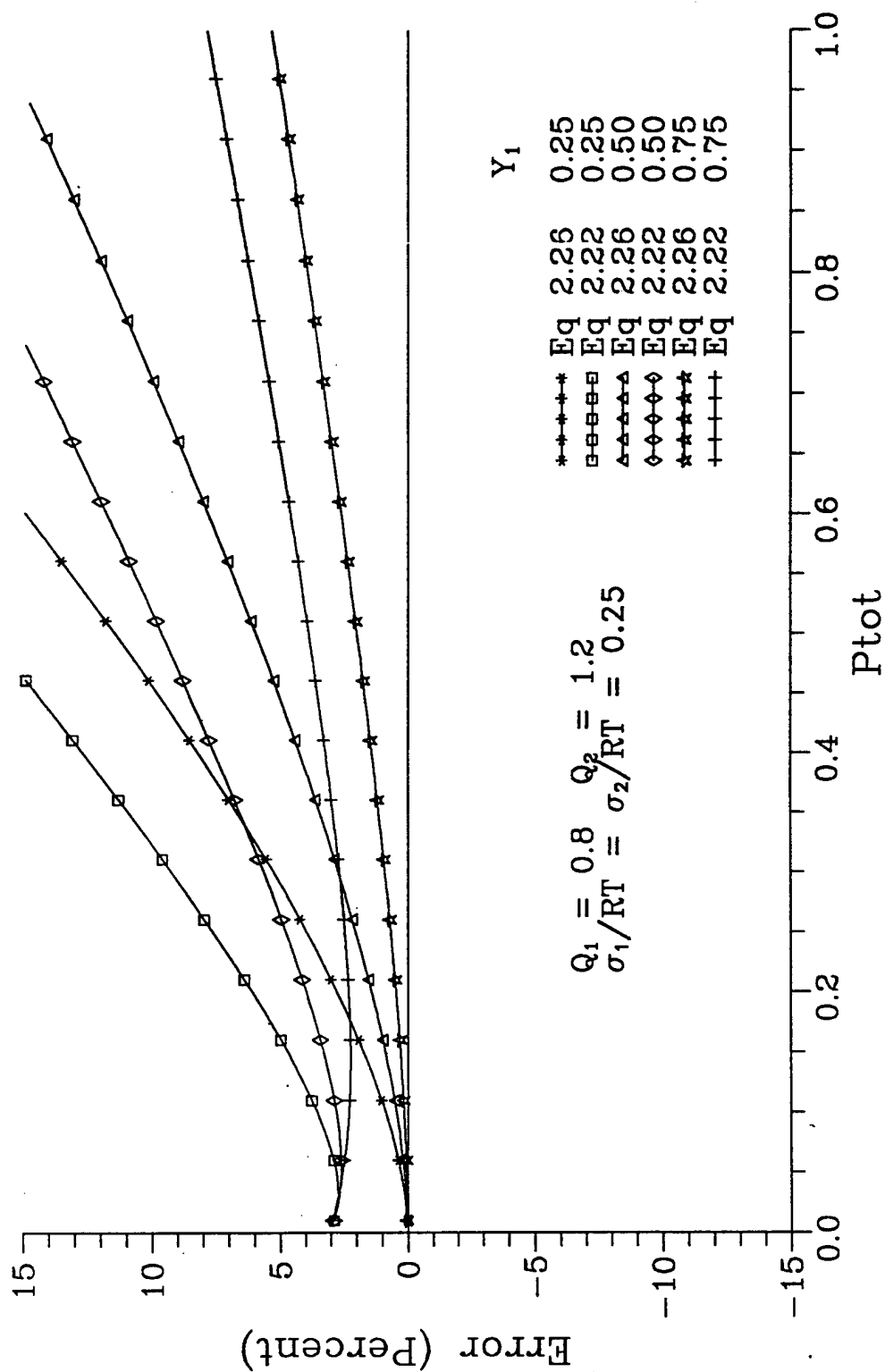25

FIGURE 2.10: Percent Error Equations 2.22 and 2.26

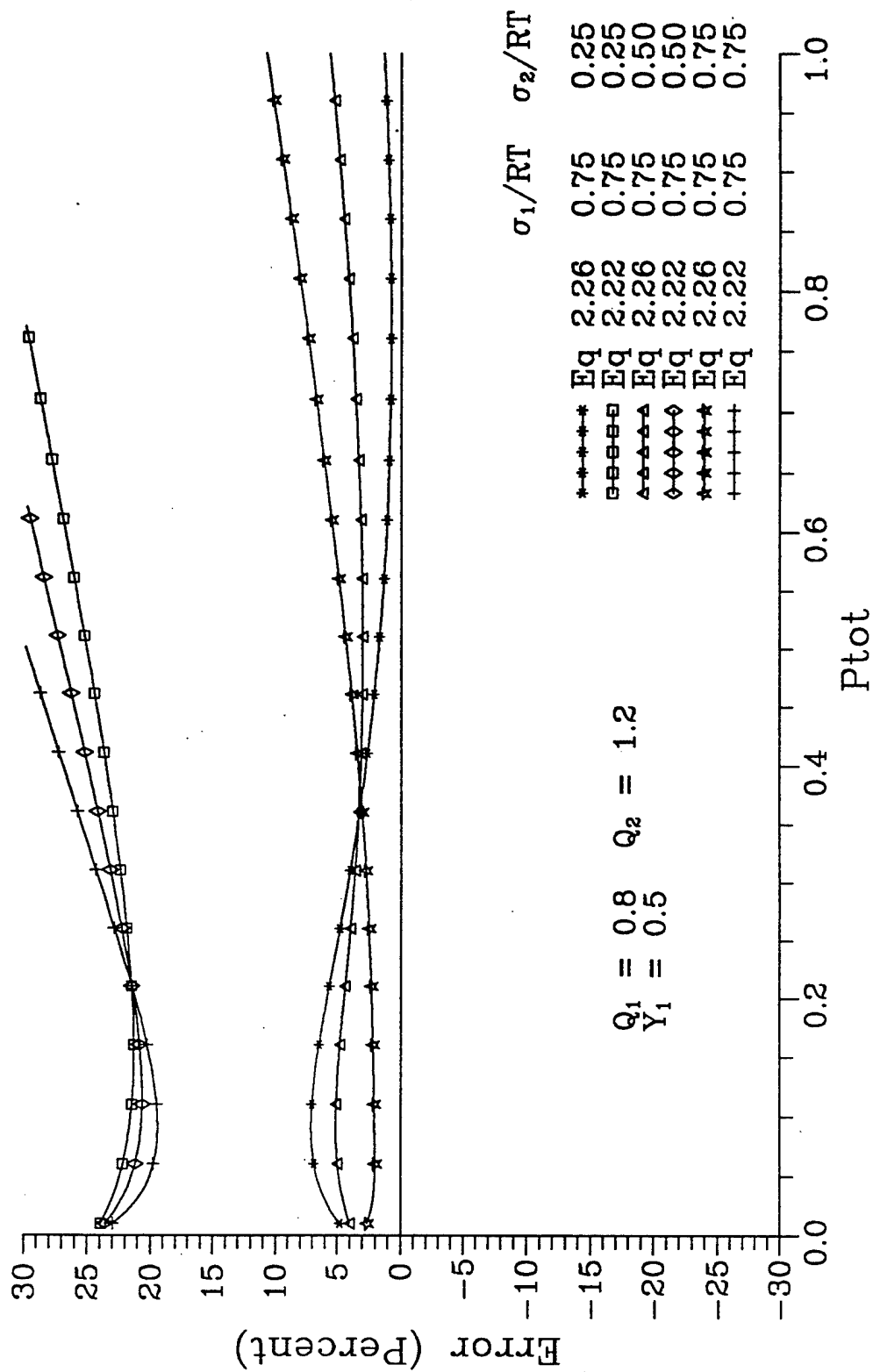FIGURE 2.11: Percent Error Equations 2.22 and 2.26

FIGURE 2.12: Percent Error Equations 2.22 and 2.26

definite error patterns develop which are consistent for both the Equation 2.22 and Equation 2.26 solutions. The major difference between the two solutions is that the Equation 2.26 solution consistently provides a corrective offset. This offset makes the Equation 2.26 solution significantly superior (as much as an order of magnitude) to the Equation 2.22 solution. In addition, as would be expected for a Taylor series expansion solution, as the spread in Q values widens, the solutions for both equations become less accurate and more divergent. It is expected that this trend would continue if mixtures demonstrating larger differences in Q values were investigated.

$\rho=1$ — **Perfect Positive Correlation**. Figures 2.13-2.18 are plots comparing Equation 2.30 results to those obtained from the homogeneous Langmuir solutions of LeVan and Vermeulen (Equation 2.22). The results from each of these equations are plotted as a percentage of error calculated from an "exact" solution. The exact solutions were generated by substituting Equations 2.9 and 2.22 into Equation 2.7 and integrating the results numerically using the Euler method. As detailed previously, the "exact" solutions are subject to the constraints inherent in Equations 2.7 and 2.22 (i.e. local Langmuir isotherm and Gaussian shaped energy distribution curves). The Euler integration was centered on $\bar{\epsilon}$ for each component using 200 integration steps. The selected model isotherm parameters are listed in Table 2.1. A copy of the BASIC code written to perform the integration, and compare the results to the calculated Equation 2.22 and Equation 2.30 results can be found in Appendix D.

The plots can be divided into two series: Figures 2.13 - 2.15 using $Q_1 = 0.9$ and $Q_2 = 1.1$, and Figures 2.16 - 2.18 using $Q_1 = 0.8$ and $Q_2 = 1.2$. As with the $\rho = 0$ case outlined above, as values for site energy distribution breadth, vapor phase mole fraction, and site energy distribution ratios are changed, definite error patterns develop which are consistent for both the Equation 2.22 and Equation 2.30 solutions. However, unlike the $\rho = 0$ case, the corrective offset provided by the heterogeneity terms inherent in the Equation 2.30 solution does not always provide a superior solution. This offset consistently shifts the homogeneous (or Equation 2.22) solutions to the more positive errors. Since the error function was defined as: moles adsorbed actual - moles adsorbed theory, positive error readings indicate that the theory is under-predicting the amount adsorbed. As the plots show, Equation 2.30 gives superior results at the lower total pressure (P_{TOT}) values. As P_{TOT} increases, both solutions drift toward more positive error readings. Thus, as P_{TOT} is increased past a threshold value, the Equation 2.30 solution becomes inferior to that of Equation 2.22.

CONCLUSIONS

As the various plots indicate, a non-iterative, heterogeneous solution has been developed that provides predictive results superior to those of analogous homogeneous solutions. Variations in the model's constituent parameters indicate that the results hold for a substantial range of conditions. The one (general) case where the new heterogeneous solution did not out-perform the homogeneous solution is rendered insignificant when the following is

29

FIGURE 2.13: Percent Error Equations 2.22 and 2.30

FIGURE 2.14: Percent Error Equations 2.22 and 2.30

31

FIGURE 2.15: Percent Error Equations 2.22 and 2.30
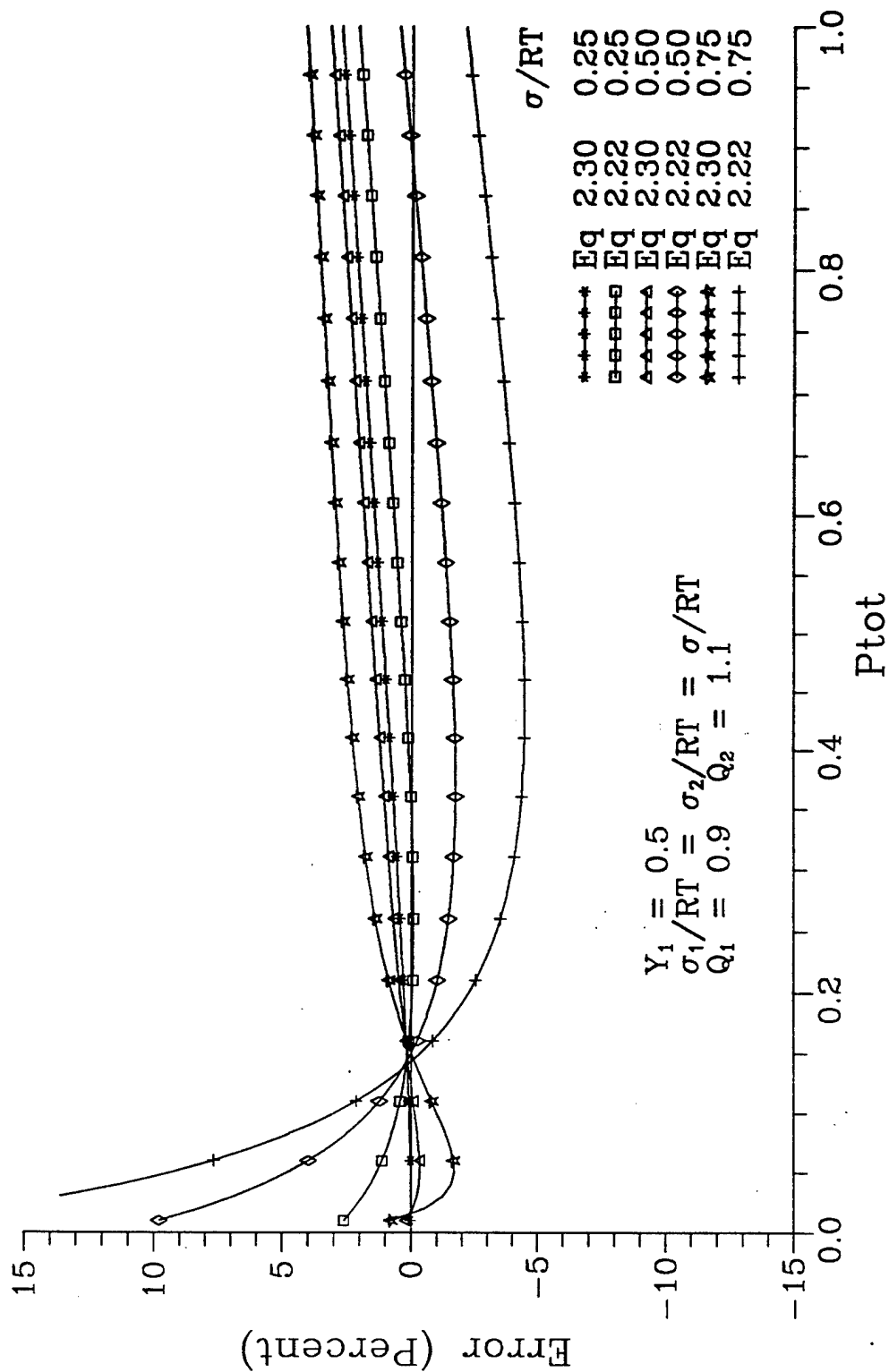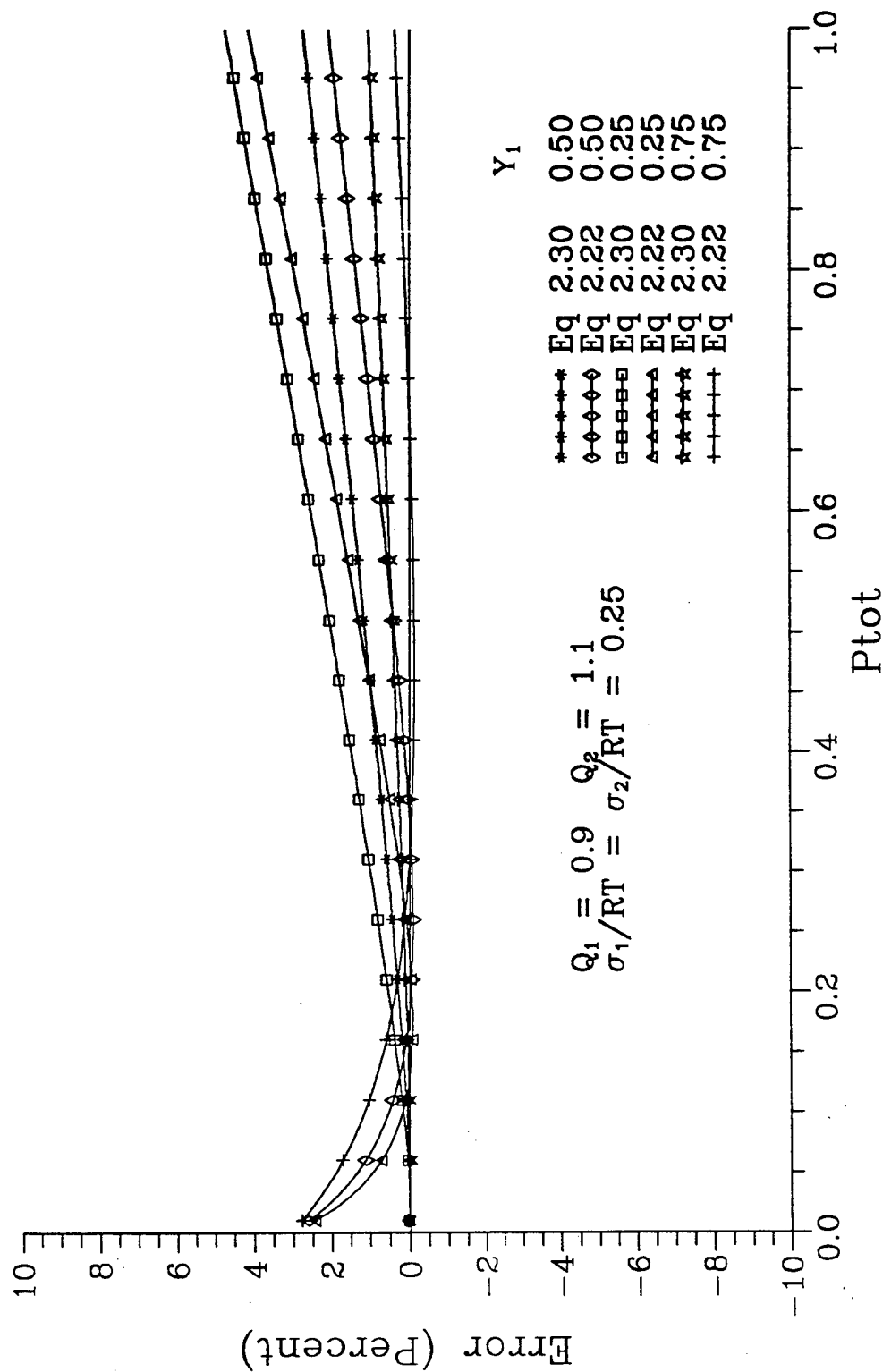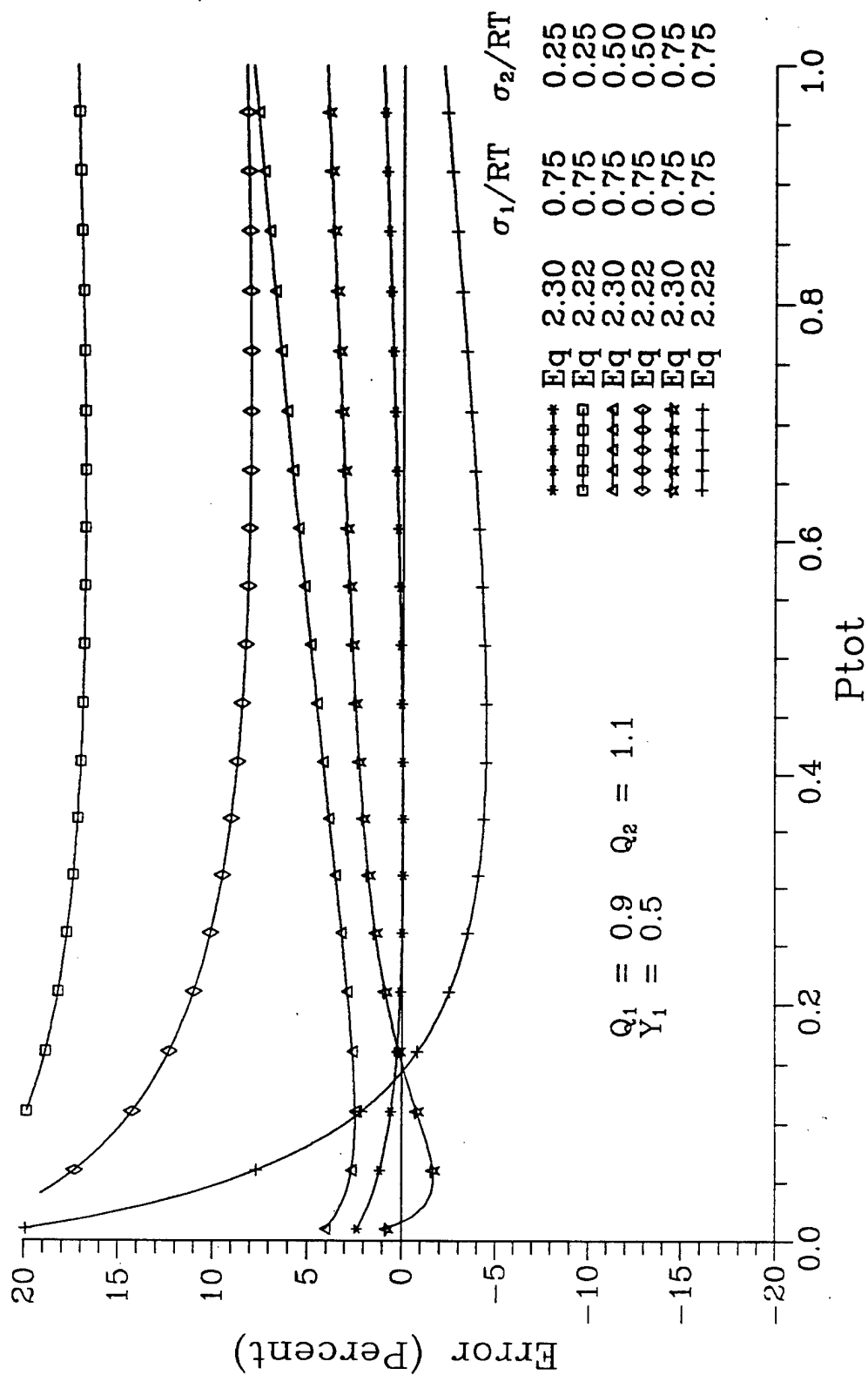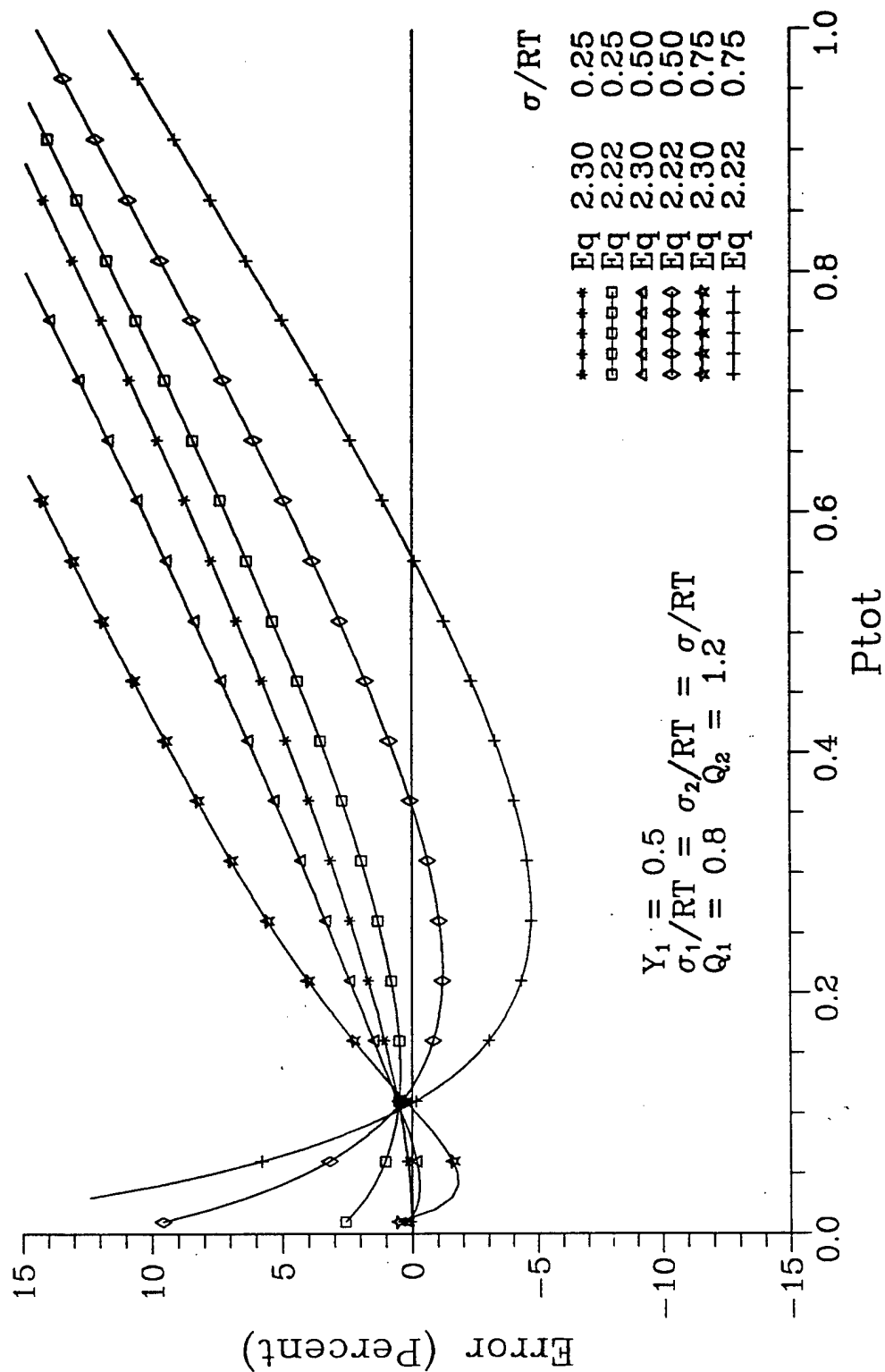
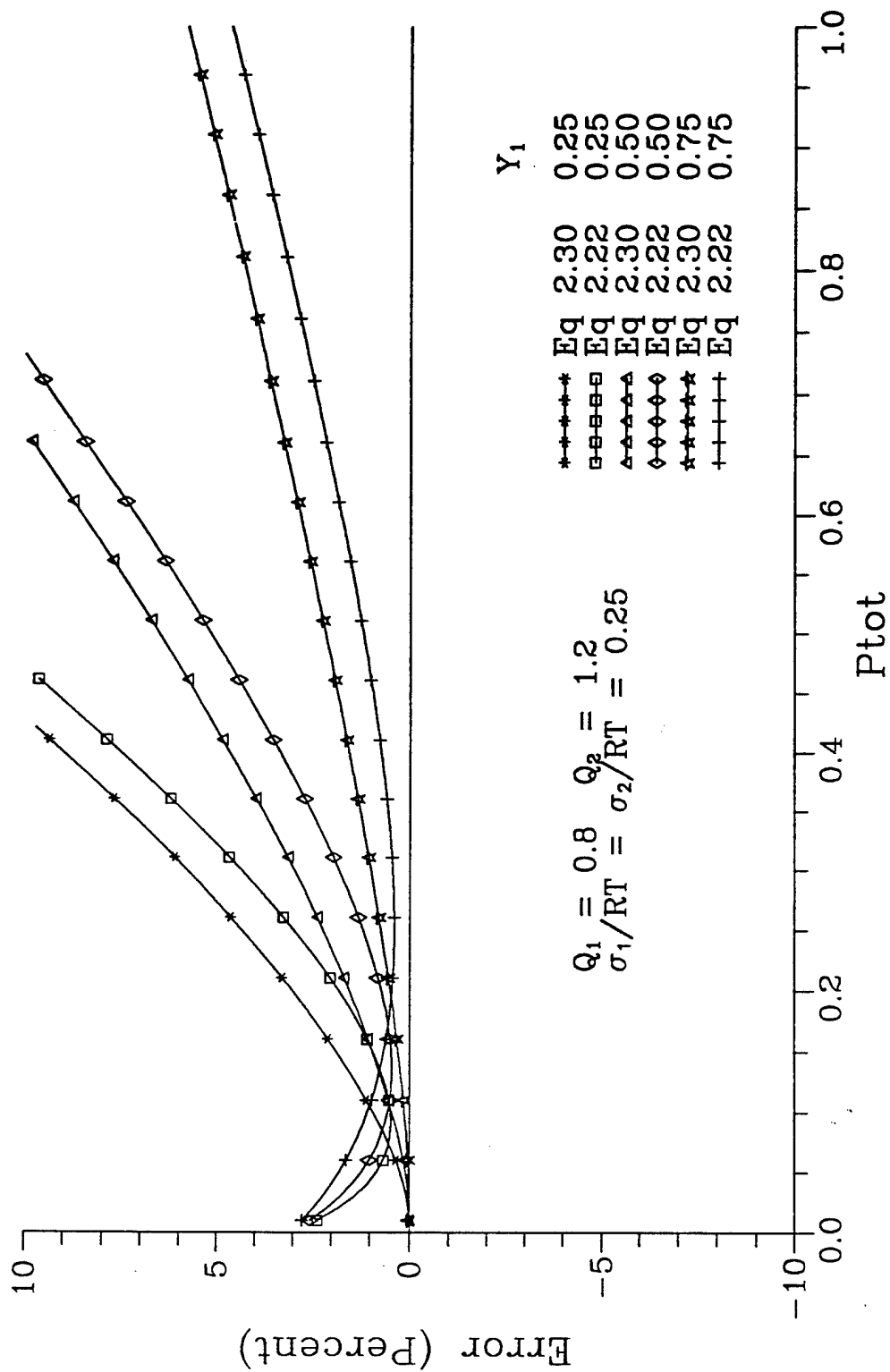FIGURE 2.16: Percent Error Equations 2.22 and 2.30

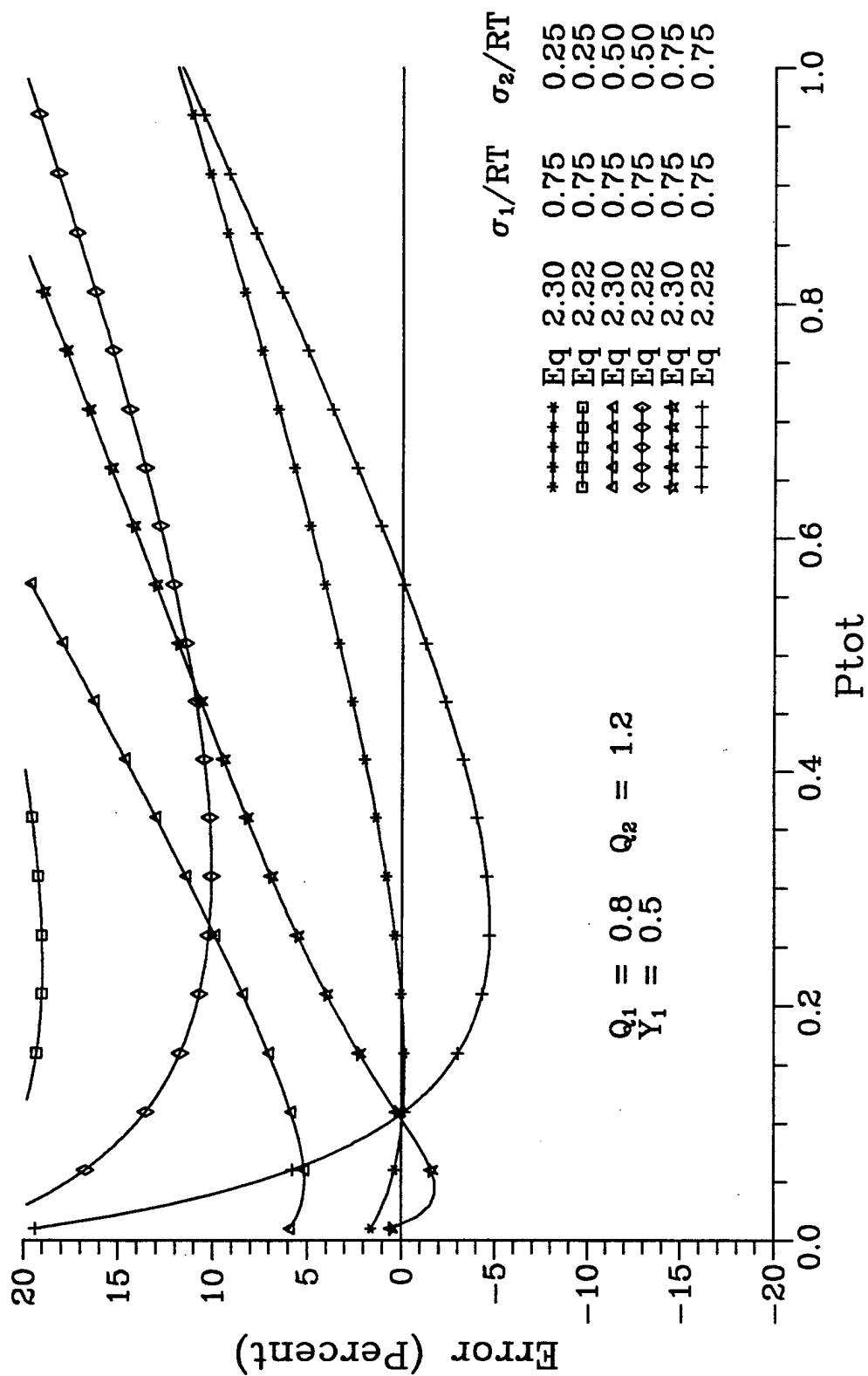FIGURE 2.17: Percent Error Equations 2.22 and 2.30

34

FIGURE 2.18: Percent Error Equations 2.22 and 2.30

35

considered: 1) the error for the fast heterogeneous model, within the range of parameters investigated, was not appreciably higher than that obtained from the homogeneous equation; 2) the parametric conditions where this occurred were limited to higher total pressures and divergent Q values; and 3) the errors for these specific cases were very low relative to the homogeneous solution errors at lower total pressures. As a result, when all conditions are considered (i.e. the full range of pressure values), the new heterogeneous model provides the most accurate solution.

An important caveat to this analysis is that the "exact" solutions which are used as error standards have inherent assumptions that may have had impact on the results. In addition, the "exact" solution is a theoretical one that is based fundamentally on a heterogeneous adsorption system. Ultimately, the utility of a developed solution is dependent on its ability to fit and predict actual mixture data.

An indication of the importance of developing fast solutions can be found in the time it took to generate the "exact" solutions in the analysis. On a relatively fast PC (80486 running at 50 MHz), the compiled code to generate 100 data points for each plot required between 10 and 200 minutes to run. This computational burden can be compared to the immeasurably short time (milliseconds or less) it takes to execute the single calculation associated with the fast heterogeneous solution. Considering that, as stated above, any isotherm subroutine in a dynamic model will be called hundreds of thousands of times, it becomes apparent that a fast model of the type developed here is desirable.

REFERENCES

Costa, E., J.L. Sotelo, G. Calleja, and C Marron, "Adsorption of Binary and Ternary Hydrocarbon Gas Mixtures on Activated Carbon: Experimental Determination and Theoretical Prediction of the Ternary Equilibrium Data", *AIChE J.* **27**, 5-12 (1981).

Frey, D. and A. Rodrigues, "Explicit Calculation of Multicomponent Equilibria for Ideal Adsorbed Solutions", *AIChE J.* **40**, 182-186 (1994).

Gamba, G., R. Rota, G. Storti, S. Carra, and M. Morbidelli, "Adsorbed Solution Theory Models for Multicomponent Adsorption Equilibria", *AIChE J.* **35**, 959-966 (1989).

Gamba, G., R. Rota, G. Storti, S. Carra, and M. Morbidelli, "Adsorption Equilibria of Nonideal Multicomponent Systems at Saturation", *AIChE J.* **36**, 1736-1742 (1990).

Hoory, S., and J. Prausnitz, "Monolayer Adsorption of Gas Mixtures on Homogeneous and Heterogeneous Solids", *Chem. Eng. Sci.* **22**, 1025-1033 (1967).

Jaroniec, M., and R. Madey, "Physical Adsorption on Heterogeneous Solids", Elsevier, New York, NY (1988).

Jaroniec, M., and W. Rudzinski, "Adsorption of Binary Gas Mixtures on Heterogeneous Surfaces", *Phys. Lett* 53A, 59-60 (1975).

LeVan, M., and T. Vermeulen, "Binary Langmuir and Freundlich Isotherms for Ideal Adsorbed Solutions", *J. Phys. Chem.* 85, 3247-3250 (1981).

Myers A., and J. Prausnitz, "Thermodynamics of Mixed-Gas Adsorption", *AIChE J.* 11, 121-127 (1965).

O'Brien, J., and A. Myers, "Physical Adsorption of Gases on Heterogeneous Surfaces", *J. Chem. Soc., Faraday Trans.* 80, 1467-1477 (1984).

O'Brien, J., and A. Myers, "Rapid Calculations of Multicomponent Adsorption Equilibria from Pure Isotherm Data", *Ind. Eng. Chem. Process Des. Dev.* 24, 1188-1191 (1985).

Talu, O., and I. Zwiebel, "Multicomponent Adsorption Equilibria of Nonideal Mixtures", *AIChE J.* 32, 1263-1276 (1986).

Valenzuela, D., A. Myers, O. Talu, and I. Zwiebel, "Adsorption of Gas Mixtures: Effect of Energetic Heterogeneity", *AIChE J.* 34, 397-402 (1988).

Van Ness, H.C. "Adsorption of Gases on Solids: Review of the Role of Thermodynamics", *I & EC Fundamentals* 8, 464-473 (1969).

APPENDIX A

BASIC code for $Q_1 = Q_2$ and $\rho = 0$

```basic
10    DEFDBL A-H, L-Z
20    DEFINT I-K
30    PI = 3.1415926#: R = 8.312440000000001D-03: ' KJ/MOLE K
40    RT = R * 298
50    DIM FX(502), GX(502)
70    INC = 200
80    GTOT1 = 0
90    INPUT "ENTER OUTPUT FILE NAME ---> ", FIL$
95    OPEN FIL$ FOR OUTPUT AS #1
100   EB1 = 10 * RT: EB2 = 12 * RT
110   B1 = EXP(-10): B2 = 1.2 * EXP(-10)
115   INPUT "ENTER SIGMA1/RT --> ", SRT1
117   INPUT "ENTER SIGMA2/RT --> ", SRT2
118   S1 = SRT1 * RT: S2 = SRT2 * RT
120   M = (S2 / S1) ^ 2
130   INPUT "ENTER GAS PHASE MOLE FRACTION Y1 ---> ", Y1
200   FOR PTOT = 0 TO 1! STEP .01
220     Q = 1
230     P1 = Y1 * PTOT
240     P2 = PTOT - P1
260     FX(0) = 0: GX(0) = 0
290     GCN = 0
295     H1 = 2 * EB1 / INC: H2 = 2 * EB2 / INC
300     FOR I = 1 TO INC
310       E1 = H1 * I
320       XS = P1 * B1 * EXP(E1 / RT)
325       PSI1 = (E1 - EB1) / S1
340       G1 = EXP(-(PSI1 ^ 2) / 2) / (S1 * (2 * PI) ^ .5)
345       FCN = 0
350       FOR J = 1 TO INC
360         E2 = H2 * J
370         YS = P2 * B2 * EXP(E2 / RT)
390         PSI2 = (E2 - EB2) / S2
500         N1 = Q * XS / (1 + XS + YS)
520         G2 = EXP(-(PSI2 ^ 2) / 2) / (S2 * (2 * PI) ^ .5)
530         IF (PTOT=0) AND (I=1) THEN GTOT2 = GTOT2 + G2 * H2: GOTO 600
550         FX(J) = N1 * G2 / GTOT2
560         IF (J = INC) THEN FCN = FCN + H2 * FX(J) / 3: GOTO 600
580         FCN = FCN + H2 * ((2 + 2 * (J MOD 2)) * FX(J)) / 3
600       NEXT J
630       IF (PTOT = 0) THEN GTOT1 = GTOT1 + G1 * H1: GOTO 790
650       GX(I) = FCN * G1 / GTOT1
660       IF (I = INC) THEN GCN = GCN + H1 * GX(I) / 3: GOTO 790
680       GCN = GCN + H1 * ((2 + 2 * (I MOD 2)) * GX(I)) / 3
790     NEXT I
800     X = P1 * B1 * EXP(EB1 / RT)
810     Y = P2 * B2 * EXP(EB2 / RT)
820     XI = 1 + X + Y
850     HH = X * (1+Y) * (1-X+Y) * S1 ^ 2 + X * Y * (Y-X-1) * S2 ^ 2
880     HX1 = Q * (X / XI + HH / (2 * XI ^ 3 * RT ^ 2))
890     LANG = Q * X / XI
895     IF (FCN = 0) THEN GOTO 920
900     DEL = (GCN - HX1) * 100 / FCN
910     DEL2 = (GCN - LANG) * 100 / FCN
920     PRINT USING "###.#### "; PTOT; GCN; HX1; DEL; LANG; DEL2; GTOT1; GTOT2
930     PRINT #1, USING "###.####### "; PTOT; DEL; DEL2
940   NEXT PTOT
945   CLOSE #1
950   END
```

APPENDIX B

BASIC code for $Q_1 = Q_2$ and $\rho = 1$

```
10   DEFDBL A-H, L-Z
20   DEFINT I-K
30   PI = 3.1415926#: R = 8.312440000000001D-03: ' KJ/MOLE K
40   RT = R * 298
50   DIM FX(5002)
70   INC = 1000
80   GTOT = 0
90   INPUT "ENTER OUTPUT FILE NAME ---> ", FIL$
95   OPEN FIL$ FOR OUTPUT AS #1
100  EB1 = 10 * RT: EB2 = 12 * RT
110  B1 = EXP(-10): B2 = 1.2 * EXP(-10)
115  INPUT "ENTER SIGMA1/RT --> ", SRT1
117  INPUT "ENTER SIGMA2/RT --> ", SRT2
118  S1 = SRT1 * RT: S2 = SRT2 * RT
120  M = (S2 / S1) ^ 2
130  INPUT "ENTER GAS PHASE MOLE FRACTION Y1 ---> ", Y1
200  FOR PTOT = 0 TO 1! STEP .01
220    Q = 1
230    P1 = Y1 * PTOT
240    P2 = PTOT - P1
260    FX(0) = 0
290    FCN = 0
295    H = 2 * EB1 / INC
300    FOR I = 1 TO INC
320      E1 = 2 * EB1 * I / INC
340      E2 = M * (E1 - EB1) + EB2
345      IF (E2 < 0) THEN PRINT "E2 < 0 ERROR": END
350      XS = P1 * B1 * EXP(E1 / RT)
360      YS = P2 * B2 * EXP(E2 / RT)
380      PSI1 = (E1 - EB1) / S1
390      PSI2 = (E2 - EB2) / S2
500      N1 = Q * XS / (1 + XS + YS)
510      G1 = EXP(-(PSI1 ^ 2) / 2) / (S1 * (2 * PI) ^ .5)
520      G2 = EXP(-(PSI2 ^ 2) / 2) / (S2 * (2 * PI) ^ .5)
530      IF (PTOT = 0) THEN GTOT = GTOT + G1 * H: GOTO 700
550      FX(I) = N1 * G1 / GTOT
560      IF (I = INC) THEN FCN = FCN + H * FX(I) / 3: GOTO 700
580      FCN = FCN + H * ((2 + 2 * (I MOD 2)) * FX(I)) / 3
700    NEXT I
800    X = P1 * B1 * EXP(EB1 / RT)
810    Y = P2 * B2 * EXP(EB2 / RT)
820    XI = 1 + X + Y
850    HH = 1 - (3*X + M*Y*(M+2)) / XI + (2*(X+M*Y) ^ 2) / XI ^ 2
880    HX1 = Q * (X / XI + (X * HH * S1 ^ 2) / (2 * XI * RT ^ 2))
890    LANG = Q * X / XI
895    IF (FCN = 0) THEN GOTO 920
900    DEL = (FCN - HX1) * 100 / FCN
910    DEL2 = (FCN - LANG) * 100 / FCN
920    PRINT USING "###.#####   "; PTOT; FCN; HX1; DEL; LANG; DEL2; GTOT
930    PRINT #1, USING "###.#######   "; PTOT; DEL; DEL2
940    NEXT PTOT
945  CLOSE #1
950  END
```

APPENDIX C

BASIC code for $Q_1 \neq Q_2$ and $\rho = 0$

```
10    DEFDBL A-H, K-Z
20    DEFINT I-J
25    DX = .0000000001#
30    PI = 3.1415926#: R = 8.312440000000001D-03: ' KJ/MOLE K
40    RT = R * 298
50    DIM FX(202), GX(202)
70    INC = 200
80    GTOT1 = 0: GTOT2 = 0
90    INPUT "ENTER OUTPUT FILE NAME ---> ", FIL$
100   EB1 = 10 * RT: EB2 = 12 * RT
110   B1 = EXP(-10): B2 = 1.2 * EXP(-10)
112   INPUT "ENTER SIGMA1/RT ---> ", SRT1
113   INPUT "ENTER SIGMA2/RT ---> ", SRT2
115   INPUT "ENTER Q1 --> ", Q1
117   INPUT "ENTER Q2 --> ", Q2
118   S1 = SRT1 * RT: S2 = SRT2 * RT
120   M = (S2 / S1) ^ 2
130   INPUT "ENTER GAS PHASE MOLE FRACTION Y1 ---> ", Y1
200   FOR PTOT = 0 TO 1! STEP .01
210     OPEN FIL$ FOR APPEND AS #1
230     P1 = Y1 * PTOT
240     P2 = PTOT - P1
260     FX(0) = 0: GX(0) = 0
290     GCN = 0
295     H1 = 2 * EB1 / INC: H2 = 2 * EB2 / INC
300     FOR I = 1 TO INC
310       E1 = H1 * I
320       XS = P1 * B1 * EXP(E1 / RT)
325       PSI1 = (E1 - EB1) / S1
340       G1 = EXP(-(PSI1 ^ 2) / 2) / (S1 * (2 * PI) ^ .5)
345       FCN = 0
350       FOR J = 1 TO INC
360         E2 = H2 * J
370         YS = P2 * B2 * EXP(E2 / RT)
390         PSI2 = (E2 - EB2) / S2
500         GOSUB 2000
520         G2 = EXP(-(PSI2 ^ 2) / 2) / (S2 * (2 * PI) ^ .5)
530         IF (PTOT = 0) AND (I = 1) THEN GTOT2 = GTOT2 + G2 * H2: GOTO 600
550         FX(J) = N1 * G2 / GTOT2
560         IF (J = INC) THEN FCN = FCN + H2 * FX(J) / 3: GOTO 600
580         FCN = FCN + H2 * ((2 + 2 * (J MOD 2)) * FX(J)) / 3
600       NEXT J
630       IF (PTOT = 0) THEN GTOT1 = GTOT1 + G1 * H1: GOTO 790
650       GX(I) = FCN * G1 / GTOT1
660       IF (I = INC) THEN GCN = GCN + H1 * GX(I) / 3: GOTO 790
680       GCN = GCN + H1 * ((2 + 2 * (I MOD 2)) * GX(I)) / 3
790     NEXT I
795     IF (PTOT = 0) THEN HX1 = 0: LANG = 0: PRINT GTOT1, GTOT2: GOTO 940
800     X = P1 * B1 * EXP(EB1 / RT)
810     Y = P2 * B2 * EXP(EB2 / RT)
820     XI = 1 + X + Y
830     QB = (Q1 * X + Q2 * Y) / (X + Y)
835     DL2 = (Q1 - Q2) * X * Y * LOG(XI) / (X + Y) ^ 2
855     A = 3 * X ^ 2 * (Q1 - QB) / ((X + Y) * XI) + 2 * X ^ 3 * (QB - Q1)
          / ((X + Y) ^ 2 * XI) + 2 * X ^ 3 * (QB - Q1) / ((X + Y) * XI ^ 2)
          + QB * X / XI - 3 * QB * X ^ 2 / XI ^ 2 + 2 * QB * X ^ 3 / XI ^ 3
860     B = X * Y * (Q2 - QB) / ((X + Y) * XI) + 2 * X * Y ^ 2 * (QB - Q2)
          / ((X + Y) ^ 2 * XI) + 2 * X * Y ^ 2 * (QB - Q2) / ((X + Y) * XI
          ^ 2) - QB * X * Y / XI ^ 2 + 2 * QB * X * Y ^ 2 / XI ^ 3
865     G = (S1 ^ 2 + S2 ^ 2) * LOG(XI) + (X * S1 ^ 2 + Y * S2 ^ 2) * (3 /
```

43

```
           XI - 6 * LOG(XI) / (X + Y)) + (X ^ 2 * S1 ^ 2 + Y ^ 2 * S2 ^ 2) *
           (6 * LOG(XI) / (X + Y) ^ 2 - 4 / ((X + Y) * XI) - 1 / XI ^ 2)
870    '
875    HH = (Q1 - Q2) * X * Y / (2 * RT ^ 2 * (X + Y) ^ 2)
880    HX1 = QB * X / XI + DL2 + S1 ^ 2 * (A + B) / (2 * RT ^ 2) + G * HH
890    LANGL = QB * X / XI + DL2
895    IF (GCN = 0) THEN GOTO 920
900    DEL = (GCN - HX1) * 100 / GCN
910    DEL2 = (GCN - LANGL) * 100 / GCN
915    DEL3 = (GCN - ((Q1 + Q2) / 2) * X / XI) * 100 / GCN
920    PRINT USING "###.##### "; PTOT; GCN; HX1; DEL; LANGL; DEL2; DEL3
930    PRINT #1, USING "###.#######   "; PTOT; DEL; DEL2; DEL3
940    CLOSE #1
945    NEXT PTOT
950 END
960 '
970 '
2000 ' LANGMUIR AST ALGORITHM
2100 '
2110 '
2115 IF (PTOT = 0) THEN N1 = 0: RETURN
2120 K1 = B1 * EXP(E1 / RT)
2130 K2 = B2 * EXP(E2 / RT)
2200 IC = 0
2210 PSI = .0000001
2220 FOR IJ = 0 TO 1 STEP 1
2230    PSIG = PSI * (1 + DX * IJ)
2240    P10 = (EXP(PSIG / Q1) - 1) / K1
2250    P20 = (EXP(PSIG / Q2) - 1) / K2
2260    X1 = P1 / P10
2270    X2 = P2 / P20
2280    IF (IJ = 0) THEN ER1 = X1 + X2 - 1 ELSE DER1 = X1 + X2 - 1
2300    NEXT IJ
2310 IF (ABS(ER1) < DX * 1000) THEN GOTO 2500
2320 IC = IC + 1
2330 IF (IC > 50) THEN PRINT "NON CONVERGE": END
2340 DDER1 = (DER1 - ER1) / (PSI * DX)
2350 PSI = PSI - ER1 / DDER1
2400 GOTO 2220
2420 '
2450 '
2470 '
2500 N10 = Q1 * K1 * P10 / (1 + K1 * P10)
2510 N20 = Q2 * K2 * P20 / (1 + K2 * P20)
2520 NTOT = 1 / (X1 / N10 + X2 / N20)
2530 N1 = NTOT * X1
2550 '
2600 RETURN
```

APPENDIX D

BASIC code for $Q_1 \neq Q_2$ and $\rho = 1$

```
10    DEFDBL A-H, K-Z
20    DEFINT I-J
25    DX = .0000000001#
30    PI = 3.1415926#: R = 8.312440000000001D-03: ' KJ/MOLE K
40    RT = R * 298
50    DIM FX(500)
70    INC = 200
80    GTOT = 0
90    INPUT "ENTER OUTPUT FILE NAME ---> ", FIL$
95    OPEN FIL$ FOR OUTPUT AS #1
100   EB1 = 10 * RT: EB2 = 12 * RT
110   B1 = EXP(-10): B2 = 1.2 * EXP(-10)
112   INPUT "ENTER SIGMA1/RT ---> ", SRT1
113   INPUT "ENTER SIGMA2/RT ---> ", SRT2
115   INPUT "ENTER Q1 --> ", Q1
117   INPUT "ENTER Q2 --> ", Q2
118   S1 = SRT1 * RT: S2 = SRT2 * RT
120   M = (S2 / S1) ^ 2
130   INPUT "ENTER GAS PHASE MOLE FRACTION Y1 ---> ", Y1
200   FOR PTOT = 0 TO 1! STEP .01
230     P1 = Y1 * PTOT
240     P2 = PTOT - P1
260     FX(0) = 0
290     FCN = 0
295     H = 2 * EB1 / INC
300     FOR I = 1 TO INC
320       E1 = H * I
340       E2 = M * (E1 - EB1) + EB2
345       IF (E2 < 0) THEN PRINT "E2 < 0 ERROR": END
350       XS = P1 * B1 * EXP(E1 / RT)
360       YS = P2 * B2 * EXP(E2 / RT)
380       PSI1 = (E1 - EB1) / S1
390       PSI2 = (E2 - EB2) / S2
500       GOSUB 2000
510       G1 = EXP(-(PSI1 ^ 2) / 2) / (S1 * (2 * PI) ^ .5)
520       G2 = EXP(-(PSI2 ^ 2) / 2) / (S2 * (2 * PI) ^ .5)
530       IF (PTOT = 0) THEN GTOT = GTOT + G1 * H: GOTO 700
550       FX(I) = N1 * G1 / GTOT
560       IF (I = INC) THEN FCN = FCN + H * FX(I) / 3: GOTO 700
580       FCN = FCN + H * ((2 + 2 * (I MOD 2)) * FX(I)) / 3
700     NEXT I
750   IF (PTOT = 0) THEN HX1 = 0: LANG = 0: GOTO 920
800   X = P1 * B1 * EXP(EB1 / RT)
810   Y = P2 * B2 * EXP(EB2 / RT)
820   XI = 1 + X + Y
830   QB = (Q1 * X + Q2 * Y) / (X + Y)
835   DL2 = (Q1 - Q2) * X * Y * LOG(XI) / (X + Y) ^ 2
840   QBP = ((Q1 * X + Q2 * M * Y) - QB * (X + M * Y)) / (X + Y)
850   QBPP = ((Q1*X+Q2*Y*M^2) - QB*(X+Y*M^2) - 2*(X+M*Y)*QBP)/(X + Y)
855   A = (QB + QBP) * (1 - 2 * (X + M * Y) / XI) + (QBP + QBPP) - QB *
      (X + Y * M ^ 2) / XI + (2 * QB * (X + M * Y) ^ 2) / (XI ^ 2)
860   B = M * ((M + 1) ^ 2) * LOG(XI) + ((X + Y * M ^ 2) + 2 * (X + M *
      Y) * (M + 1)) / XI
865   G = ((X + M * Y) ^ 2) / (XI ^ 2) + (4 * (X + M * Y) ^ 2) / ((X +
      Y) * XI) + 2 * M * (2 * X + 3 * M * Y - Y) * LOG(XI) / (X + Y)
870   '
875   HH = X * A / XI + (Q1 - Q2) * X * Y * (B - G) / ((X + Y) ^ 2)
880   HX1 = QB * X / XI + DL2 + S1 ^ 2 * HH / (2 * RT ^ 2)
890   LANGL = QB * X / XI + DL2
895   IF (FCN = 0) THEN GOTO 920
```

```
900    DEL = (FCN - HX1) * 100 / FCN
910    DEL2 = (FCN - LANGL) * 100 / FCN
915    DEL3 = (FCN - ((Q1 + Q2) / 2) * X / XI) * 100 / FCN
920    PRINT USING "###.##### ";PTOT;FCN;HX1;DEL;LANGL;DEL2;GTOT;DEL3
930    PRINT #1, USING "###.#######   "; PTOT; DEL; DEL2; DEL3
940    NEXT PTOT
945 CLOSE #1
950 END
960 '
970 '
2000 ' LANGMUIR AST ALGORITHM
2100 '
2110 '
2115 IF (PTOT = 0) THEN N1 = 0: RETURN
2120 K1 = B1 * EXP(E1 / RT)
2130 K2 = B2 * EXP(E2 / RT)
2200 IC = 0
2210 PSI = .0000001
2220 FOR IJ = 0 TO 1 STEP 1
2230    PSIG = PSI * (1 + DX * IJ)
2240    P10 = (EXP(PSIG / Q1) - 1) / K1
2250    P20 = (EXP(PSIG / Q2) - 1) / K2
2260    X1 = P1 / P10
2270    X2 = P2 / P20
2280    IF (IJ = 0) THEN ER1 = X1 + X2 - 1 ELSE DER1 = X1 + X2 - 1
2300    NEXT IJ
2310 IF (ABS(ER1) < DX * 1000) THEN GOTO 2500
2320 IC = IC + 1
2330 IF (IC > 50) THEN PRINT "NON CONVERGE": END
2340 DDER1 = (DER1 - ER1) / (PSI * DX)
2350 PSI = PSI - ER1 / DDER1
2400 GOTO 2220
2420 '
2450 '
2470 '
2500 N10 = Q1 * K1 * P10 / (1 + K1 * P10)
2510 N20 = Q2 * K2 * P20 / (1 + K2 * P20)
2520 NTOT = 1 / (X1 / N10 + X2 / N20)
2530 N1 = NTOT * X1
2550 '
2600 RETURN
```